

STATUS OF THESIS

Title of thesis

SPRAY CHARACTERISTICS AND SPRAY-WALL IMPINGEMENT
OF A DIESEL-CNG DUAL FUEL JET USING THE SCHLIEREN
IMAGING TECHNIQUE

I MHADI ABAKER ISMAEL HARROUN

hereby allow my thesis to be placed at the Information Resource Center (IRC) of Universiti Teknologi PETRONAS (UTP) with the following conditions:

1. The thesis becomes the property of UTP
2. The IRC of UTP may make copies of the thesis for academic purposes only.
3. This thesis is classified as

☐ Confidential

☒ Non-confidential

If this thesis is confidential, please state the reason:

The contents of the thesis will remain confidential for _____ years.

Remarks on disclosure:

Signature of Author



Permanent address: _____

Bahari University

College of Engineering

Khartoum-Sudan

Date : 30/8/13

Endorsed by

Ir. Dr. Masri Baharom
Head of Department/Associate Profes
Department of Mechanical Engineering,
Universiti Teknologi PETRONAS
Bandar Seri Iskandar, 31750 Tronoh,
Perak Darul Ridzuan, Malaysia

Signature of Supervisor

Name of Supervisor

Prof. Dr. Morgan R. Heikal

Date : 2/9/13

UNIVERSITI TEKNOLOGI PETRONAS

SPRAY CHARACTERISTICS AND SPRAY-WALL IMPINGEMENT OF A

DIESEL-CNG DUAL FUEL JET USING THE SCHLIEREN IMAGING

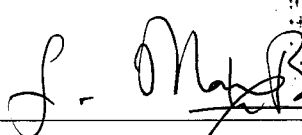
TECHNIQUE

by

MHADI ABAKER ISMAEL HARROUN

The undersigned certify that they have read, and recommend to the Postgraduate Studies Programme for acceptance this thesis for the fulfillment of the requirements for the degree stated.

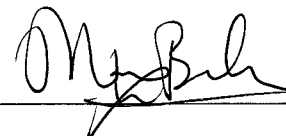
Signature:


Ir. Dr. Masri Baharom
Head of Department/Associate Professor
Department of Mechanical Engineering
Universiti Teknologi PETRONAS
Bandar Seri Iskandar, 31750 Tronoh,
Perak Darul Ridzuan, Malaysia

Main Supervisor:

Prof. Dr. Morgan R. Heikal


Signature:


Ir. Dr. Masri Baharom
Head of Department/Associate Professor
Department of Mechanical Engineering
Universiti Teknologi PETRONAS
Bandar Seri Iskandar, 31750 Tronoh,
Perak Darul Ridzuan, Malaysia

Co-Supervisor:

Assoc. Prof. Ir. Dr. Masri B. Baharom

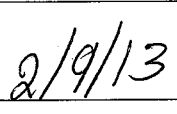
Signature:


Ir. Dr. Masri Baharom
Head of Department/Associate Professor
Department of Mechanical Engineering
Universiti Teknologi PETRONAS
Bandar Seri Iskandar, 31750 Tronoh,
Perak Darul Ridzuan, Malaysia

Head of Department:

Assoc. Prof. Ir. Dr. Masri B. Baharom

Date:


2/9/13

SPRAY CHARACTERISTICS AND SPRAY-WALL IMPINGEMENT OF A
DIESEL-CNG DUAL FUEL JET USING THE SCHLIEREN IMAGING
TECHNIQUE

by

MHADI ABAKER ISMAEL HARROUN

A Thesis

Submitted to the Postgraduate Studies Programme

as a Requirement for the Degree of

MASTER OF SCIENCE

MECHANICAL DEPARTMENT

UNIVERSITI TEKNOLOGI PETRONAS

BANDAR SERI ISKANDAR,

PERAK

SEPTEMBER 2013

DECLARATION OF THESIS

Title of thesis

SPRAY CHARACTERISTICS AND SPRAY-WALL IMPINGEMENT
OF A DIESEL-CNG DUAL FUEL JET USING THE SCHLIEREN
IMAGING TECHNIQUE

I MHADI ABAKER ISMAEL HARROUN

hereby declare that the thesis is based on my original work except for quotations and citations which have been duly acknowledged. I also declare that it has not been previously or concurrently submitted for any other degree at UTP or other institutions.

Signature of Author



Permanent address: _____

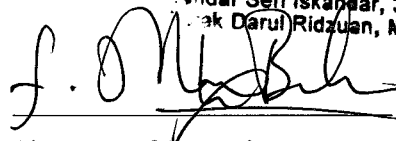
Bahri University

College of Engineering

Khartoum-Sudan

Date : 02-08-2013

Witnessed by **Ir. Dr. Masri Baharom**
Head of Department/Associate Professor
Department of Mechanical Engineering
Universiti Teknologi PETRONAS
Pandak Seri Iskandar, 31750 Tronoh,
Pangkalankanan Darul Ridzuan, Malaysia



Signature of Supervisor

Name of Supervisor

Prof. Dr. Morgan R Heikal

Date : 02-09-2013

DEDICATION

I would like to dedicate my thesis to my family especially for my beloved parents for giving birth to me at the first place and who taught me that “The knowledge is the key to Success”.

ACKNOWLEDGEMENTS

First and foremost, I would like to give my sincere thanks to Allah who gave me the strength to complete this work.

I would like to express my sincere gratitude to my supervisor Prof. Dr. Morgan Remond Heikal for continuous support of my study and research, for his patience, motivation, enthusiasm, and immense knowledge. His guidance helped me in all the time of research and writing of this thesis.

I would like to thank my co-supervisor Assoc. Prof. Ir. Dr. Masri Bin Baharoom, for guiding me, helping me through thesis writing, and also for his kindness and helping whenever necessary.

My sincere thanks also goes to Mr. Saiful Azrin B Mohd Zulkifli on helping us building the LABVIEW program.

Also I would like to thank my fellow labmates in the automotive research center: Mr. Firmansyah, Mr. Ftwi, Mr. Saheed, Mr. Wasiuayan and Mr. M. Alamen for their help and assistance.

Last but not the least, I would like to thank my parents for giving birth to me at the first place and supporting me spiritually throughout my life.

ABSTRACT

Natural gas for direct-injection (DI) compression ignition (CI) engines is considered to be the final optimized method due to its high volumetric efficiency, high thermal efficiency and low emissions. However, CNG has the penalty of high auto-ignition temperature and lower cetane number. An effective way to use CNG in CI engines is to inject the CNG with a pilot of diesel fuel for ignition purposes. In order to understand and control the injection and the jet characteristics, it is essential to understand how the gas jets assist the atomization of the pilot diesel spray and influence its characteristics as well as wall impingement.

This research is an experimental investigation of the direct injection of CNG jet, diesel spray and combination of fuels (i.e. natural gas with pilot of diesel fuel) in a constant volume chamber using an optical method. The jets were created using two parallel injectors. A low pressure CNG injector (electronic) was used at different injection pressures ranging from 14 bar to 18 bar, while a diesel sprayed injector was used for a high pressure common rail injector ranging from 500 to 700 bar.

The Schlieren technique was used for flow visualization and a high speed video camera was used for image acquisition. Series of images of a jet at different time intervals from the beginning of the injection were taken to determine the macroscopic characteristics such as jet penetration rate, jet cone angle and jet tip velocity. The jet radial and height travel along the wall under different injection pressures and temperatures were also measured. Image processing software was developed and used for the analysis.

The optically observed macroscopic characteristics of the CNG jet were largely affected by the ambient air at the start of injection in comparison with diesel spray. The diesel-CNG dual-fuel macroscopic characteristics were compared to the pure diesel spray at the same conditions and threshold values. The jet penetration rate was

observed to be higher in the diesel-CNG dual-fuel case than that of the pure diesel, while the spray cone angle was found to be lower. The temperature effect on the diesel-CNG dual-fuel was not significant as in the case of pure diesel spray. The diesel spray characteristics were compared to existing calculations of spray characteristics for validation purposes. The jet-wall impingement of the diesel fuel was largely effected by the CNG jet which has resulted in a faster penetration along the wall, while the temperature effect was observed to be higher in the pure diesel spray as compared to the diesel-CNG dual-fuel.

ABSTRAK

Gas asli untuk suntikan-terus (DI) pencucuhan mampatan (CI) enjin adalah dianggap sebagai kaedah terakhir yang paling dioptimumkan kerana kecekapan isipadu yang tinggi, kecekapan haba yang tinggi dan pengeluaran yang rendah. Walau bagaimanapun, CNG mempunyai kelemahan pada suhu yang tinggi menyebabkan penyalaan automatik dan bilangan setana lebih rendah. Satu cara yang berkesan untuk menggunakan CNG dalam enjin CI adalah untuk menyuntik CNG dengan perintis bahan api diesel untuk tujuan pencucuhan. Dalam usaha untuk memahami dan mengawal suntikan dan ciri-ciri jet, adalah amat penting untuk memahami bagaimana jet gas membantu pengabusan semburan diesel perintis dan pengaruh ciri-ciri serta hentaman dinding.

Kajian ini adalah satu siasatan ujikaji suntikan langsung jet CNG, semburan diesel dan gabungan bahan api (iaitu gas asli dengan perintis bahan api diesel) dalam ruang isipadu malar menggunakan kaedah optik. Jet dicipta dengan menggunakan dua penyuntik selari. Penyuntik elektronik gas CNG dengan tekanan yang rendah telah digunakan pada tekanan suntikan yang berbeza dari 14 bar hingga 18 bar, manakala penyuntik diesel disembur penyuntik 'common rail' pada tekanan tinggi antara 500 bar hingga 700 bar.

Teknik Schlieren telah digunakan untuk mengvisualisasikan aliran bahan api dan kamera video kelajuan tinggi digunakan untuk mengambil beberapa set imej. Siri imej jet pada selang masa yang berbeza dari permulaan suntikan telah diambil untuk menentukan ciri-ciri makroskopik seperti kadar penembusan jet, sudut kon jet dan halaju hujung jet. Jejarian jet dan jarak ketinggian perjalanan sepanjang dinding dibawah tekanan suntikan yang berbeza dan suhu juga diukur. Perisian pemprosesan imej telah dibangunkan dan digunakan untuk analisis.

Ciri-ciri makroskopik jet CNG diperhatikan melalui optik dan didapati sebahagian besarnya dipengaruhi oleh udara sekeliling pada permulaan suntikan berbanding dengan semburan diesel. Ciri-ciri makroskopik Diesel-CNG dwi-bahan api dibandingkan dengan semburan diesel tulen pada keadaan yang sama dan nilai-nilai ambang. Kadar penembusan jet didapati lebih tinggi didalam kes dwi-bahan api diesel-CNG berbanding diesel tulen, manakala sudut kon semburan didapati lebih rendah. Kesan suhu ke atas diesel-CNG dwi-bahan api adalah tidak ketara jika dibandingkan dengan kes semburan diesel tulen. Ciri-ciri semburan diesel dibandingkan dengan pengiraan yang sedia ada untuk tujuan pengesahan. Hentaman jet-dinding bahan api diesel yang sebahagian besarnya dipengaruhi oleh jet CNG telah menyebabkan penembusan yang lebih cepat di sepanjang dinding, manakala kesan suhu diperhatikan lebih tinggi pada semburan diesel tulen berbanding dengan diesel-CNG dwi-bahan api.

In compliance with the terms of the Copyright Act 1987 and the IP Policy of the university, the copyright of this thesis has been reassigned by the author to the legal entity of the university,

Institute of Technology PETRONAS Sdn Bhd.

Due acknowledgement shall always be made of the use of any material contained in, or derived from, this thesis.

© September, 2013

Institute of Technology PETRONAS Sdn Bhd

All rights reserved.

TABLE OF CONTENT

ABSTRACT	vii
ABSTRAK	ix
LIST OF FIGURES	xiv
LIST OF TABLES	xvii
CHAPTER 1 INTRODUCTION	1
1.1 Research Background and Motivation	1
1.1.1 Natural Gas as an Alternative Fuel	2
1.1.2 Natural Gas in Compression-Ignition Engines (diesel engines)	2
1.2 Spray characteristics and spray-wall impingement	4
1.3 Problem statement	5
1.4 Scope of the Research	5
1.5 Research Objective	6
1.6 Outline of the Thesis	6
CHAPTER 2 LITERATURE SURVEY	8
2.1 Compressed Natural Gas as an Engine Fuel	8
2.2 Compressed Natural Gas in Spark Ignition Engine	9
2.2.1 Compressed Natural Gas in DICIEs	10
2.3 Diesel Spray Charactrestics and Spray-Wall Impingement	12
2.4 Natural Gas Jet Characteristics and Jet-Wall Impingement	14
2.5 CNG Jet and diesel spray dual injection Characteristics and Jet-Wall Impingement	16
2.6 Summary	16
CHAPTER 3 EXPERIMENTAL WORK	18
3.1 The Experimental Setup	18
3.1.1 Test Rig Design	18
3.1.2 CNG Injection System	20
3.1.2.1 CNG Composition and Properties	21
3.1.2.2 CNG Injection Measturement	22
3.1.3 Diesel Injection System	25
3.1.3.1 Diesel Injection Measturement	27
3.1.4 Control System, Data acquisition, and Triggering	28
3.1.5 Schlieren Technique	30

3.1.6 Image Processing	31
CHAPTER 4 RESULTS AND DISCUSSIONS	35
4.1 Development of the Compressed Natural Gas Jet.....	35
4.1.1 Effect of injection pressure on the CNG jet penetration.....	37
4.1.2 Effects of injection pressure on the CNG jet Cone Angle	39
4.1.3 Effect of injector-wall distance on the jet tip penetration	40
4.1.4 Effects of Wall impingement on the CNG jet development	41
4.1.5 Effect of injection pressure of CNG jet on the Wall-impingement	44
4.2 Spray Characteristics of Diesel and Diesel-CNG Dual Fuel Jet	46
4.2.1 Spray Tip Penetration Measurements	46
4.2.2 Spray tip velocity measurements	47
4.2.3 Spray cone angle measurements	49
4.2.4 Temperature effects.....	50
4.2.4.1 Spray Tip Penetration Measurement	50
4.2.4.2 Spray cone angle measurement	53
4.2.4.3 Spray tip velocity measurement	54
4.2.5 Calculations of the diesel jet characteristics	55
4.2.6 Effects of Wall impingement on the diesel-CNG dual fuel jet development.....	58
4.2.6.1 Effect of injection pressure on the radial penetration.....	60
4.2.6.2 The effect of wall distance from the injector on the jet radial penetration	61
4.2.6.3 The effect of wall temperature on the diesel and diesel-CNG dual fuel radial penetration	63
CHAPTER 5 CONCLUSIONS AND RECOMMENDATIONS	71
5.1.1 CONCLUSIONS.....	71
5.2 RECOMMENDATIONS	73
REFERENCES	74
APPENDIX A MATLAB IMAGING CODE	79

LIST OF FIGURES

Figure 1.1: Methods of Using Natural Gas in Engines.....	3
Figure 3.1: Experimental Test Rig.....	19
Figure 3.2: CNG Fuel Injection System.	21
Figure 3.3: Natural gas injector	21
Figure 3.4: The set up for the injector flow calibration.....	24
Figure 3.5: Mass Flow rate versus injection duration for different injection pressures	24
Figure 3.6: Common rail injector used for diesel spray study.....	26
Figure 3.7: Diesel Fuel Injection System	26
Figure 3.8: Effect of injection pressure on time-resolved injection rate (energizing time of the solenoid is 5ms).....	28
Figure 3.9: Injection control system	29
Figure 3.10: Lab VIEW PID loop interface and block diagram.....	30
Figure 3.11: Experimental set-up for Schlieren technique.	31
Figure 3.12: unprocessed digital spray image (a & b) and image after applying the threshold (c).....	32
Figure 3.13: Definitions of spray tip penetration and cone angle.....	33
Figure 3.14: Definitions of spray radial penetration and spray height [50].....	34
Figure 4.1: Schlieren images of spray pattern of CNG at 18 bar injection pressure and 80 mm injector to the wall distance.	36
Figure 4.2: Schlieren images for CNG jets at different injection pressures (18, 16 and 14 bar) and 80mm injector to the wall distance.....	38
Figure 4.3: The effect of injection pressure on the CNG jet tip penetration at injection pressures: 18, 16 and 14 bar, and injector wall distance: 80 mm.	39
Figure 4.4: the effect of injection pressure on the CNG jet cone angle at injection pressures: 18, 16 and 14bar.	40
Figure 4.5: The effect of the injector-wall distance on the jet tip penetration against time.	41

Figure 4.6: CNG jet-wall impingement at injection pressure: 18bar and injector to the wall distance: 40mm.	42
Figure 4.7: Concentration field of CNG jet	43
Figure 4.8: Development of the CNG jet impingement (radial penetration and jet height) along the wall versus time	44
Figure 4.9: Effects of different injection pressures (18, 16 and 14bar) along the Wall-impingement at 40mm injector to the wall distance.	45
Figure 4.10: Effects of different injection pressures (18, 16 and 14bar) on the height along the Wall-impingement at 40mm injector to the wall distance.	45
Figure 4.11: Schlieren images for diesel and diesel-CNG dual fuel at injection pressure: 600, 18 bar for diesel and CNG respectively and the injector wall distance: 80 mm.	47
Figure 4.12: Spray tip velocity of diesel and diesel-CNG dual fuel jet at injection pressure: 600 and 18 bar for diesel and CNG respectively and the injector to the wall distance: 80 mm.	48
Figure 4.13: Spray tip velocity of the diesel and the diesel-CNG dual-fuel jet at different injection pressures (700, 600 and 500 bar) for diesel spray and 18 bar for the CNG jet and injector wall distance: 80 mm.	49
Figure 4.14: Spray cone angle of diesel and diesel-CNG at injection pressure: 600, 18 bar for diesel and CNG respectively and injector wall distance: 80 mm.	50
Figure 4.15: Effect of different temperatures (500, 400 and 300 °K) on the diesel and diesel-CNG dual fuel at injection pressure: 600 and 18 bar for diesel and CNG respectively.	51
Figure 4.16: Effect of different injection pressures (500, 600 and 700 bar) on the diesel and diesel-CNG dual fuel at 500 K wall temperatures.	52
Figure 4.17: Spray cone angle of diesel and diesel-CNG dual-fuel at different wall temperatures (500, 400 and 300°K) and the injection pressure: 600bar and 18 bar diesel and the CNG respectively.	54
Figure 4.18: Spray tip velocity of diesel and diesel-CNG dual-fuel jet at different wall temperatures (500 and 300K), injection pressure: 600, 18bar for diesel and CNG respectively and injector wall distance: 80 mm.	55
Figure 4.19: Comparison between the experimental and the calculated spray tip penetration of diesel fuel at injection pressure 600bar and ambient temperature.	56

Figure 4.20: Comparison between the experimental and the calculated spray tip penetration of the diesel fuel at injection pressure 600 bar and the wall temperature 500°K.	57
Figure 4.21: Comparison between the experimental and the calculated spray tip velocity of diesel fuel at injection pressure 600 bar at ambient temperature.	58
Figure 4.22: The effects of injection pressure on the characteristics of diesel spray and diesel-CNG dual fuel impingement.	59
Figure 4.23: The radial penetration and height of diesel and diesel-CNG dual fuel jet impinged on the wall (inj. P= 600 bar for diesel and 18 bar for CNG, 60mm inj. to the wall distance and the wall temperature 400K).....	60
Figure 4.24: Effect of injection pressure on the radial penetration of diesel and diesel-CNG dual fuel impinged on the wall at diesel and CNG injection pressures 600 bar and 18 bar respectively.	61
Figure 4.25: Effect of injector-wall distance on the radial penetration of the diesel spray at injection pressure 600 bar.	62
Figure 4.26: Effect of injector-wall distance on the radial penetration of the diesel-CNG dual fuel jet at injection pressure 600 bar and 18 bar respectively.	62
Figure 4.27: Effect of wall temperature on the radial penetration of diesel-CNG dual fuel impinged on the wall at diesel and CNG injection pressures 600 bar and 18 bar respectively.	63
Figure 4.28: Effect of wall temperature on the radial penetration of diesel fuel impinged on the wall at injection pressure 600 bar.	64

LIST OF TABLES

Table 3.1: Experimental condition	22
Table 3.2: Typical Composition of the CNG in Malaysia [16]	23
Table 3.3: Fuel Properties of CNG [46]	23
Table 3.4: Properties of Diesel Fuel tested	28

CHAPTER 1

INTRODUCTION

1.1 Research Background and Motivation

A shortage of crude oil is expected during the early decades of this century, while at the same time the energy needs for the internal combustion engines are growing rapidly. Liquid hydrocarbon fuels have become the main energy sources and the primary fuel for transportation. ~~In addition, air pollution is becoming more serious~~ and tighter regulations for emissions from engines have widely become the focus of manufactures and research centers all over the world. Therefore, researchers continue to find new sources of crude oil while at the same time develop innovative technologies to reduce the dependencies on conventional fuels.

Internal combustion engines have largely contributed to the global air pollution leading to the deterioration of the environment. Correspondingly, interest is growing to develop the internal combustion engines to reduce the exhaust emissions of the regulated pollutants. In particular, the gases related the fossil fuel combustion engines are hydrocarbon (HC), carbon monoxide (CO) and nitrogen oxide (NO_x) which effect human life [1]. Therefore, the development of alternative fuels for engines has been a major concern of the researchers and manufactures since they are cleaner as compared to conventional fuels. The improvement in the fuel economy of combustion engines is quite important until new affordable alternative energy resources are found and widely used. This resulted in an increased interest to use alternative fuels in internal combustion engines.

1.1.1 Natural Gas as an Alternative Fuel

Interest in developing alternative fuel technologies for internal combustion engines began in the 1970s in response to the energy crisis and emission regulations. Natural gas (NG), and other gaseous fuels have been widely used as alternative fuels in internal combustion engines because of their potential to maintain engine performance and reduce the emissions of hydrocarbons [2]. Most of the research interest has been focused on the use of NG as an alternative fuel, mainly due to its wide availability, and low cost compared to other gaseous fuels. The high octane number of CNG also allows the engine to operate at a higher compression ratio and hence a higher thermal efficiencies. NG also has an excellent lean flammability limit allowing for lean burn operation, which reduces the production of air pollutants in the exhaust emissions and raises the thermal efficiency at part load [3].

Natural gas has been tested as an alternative fuel in a variety of engine configurations. The main engine types include spark ignition, lean burn, dual-fuel (pilot injection), and the direct compression ignition engines (DICIEs) as shown in Fig.1.1.1. Successful studies have been carried out on these engines and have shown higher thermal efficiency with lower emissions of hydrocarbon [3, 4]. However, there remains many problems facing the researchers and manufactures in designing CNG engines; these include low flame propagation speed, fuel evaporation rate, high ignition temperature, losses in volumetric efficiency, and low power output of the engine [5]. Due to these difficulties, many researchers have been considering the most promising solution, namely the direct injection of natural gas with a diesel pilot injection. However, this solution still requires further development in order to realize the advantages of diesel engines and their full potential.

1.1.2 Natural Gas in Compression-Ignition Engines (diesel engines)

In recent years, natural gas is being used increasingly in internal combustion diesel engines due to the lower costs compared to petroleum. There are different principal methods for NG to be used in compression ignition engines: the first one, the natural gas is injected into the inlet manifold, mixes naturally with the air and

forms a fully pre-mixed fuel-air mixture in the combustion chamber. Thus a mixture of gas and air is compressed during the compression stroke and before the end of the stroke; a pilot quantity of diesel fuel is injected to initiate combustion. This kind of operating condition produces a none-uniform mixture distribution of the natural gas resulting in an increase in the unburned hydrocarbon emissions at high loads [6]. While at low loads, the engine requires more fuel delivery (diesel fuel) to operate efficiently. Another drawback of this system is that it does not favor the two-stroke engine due to the escape of some of the natural gas fuel into the exhaust.

The second method of using natural gas in diesel engines is the direct injection of natural gas near to the diesel fuel spray into the combustion chamber. Thus a full stratification of the fuel-air mixture can be obtained with good flammability over the entire load range. Recently, successful operation has been demonstrated by applying this method using a prototype co-injector[7], resulting in diesel-gas two phase mixtures which were then injected into the chamber. The authors recommended that the jet penetration should be imaged and characterized to further understand the complex two-phase flow phenomena.

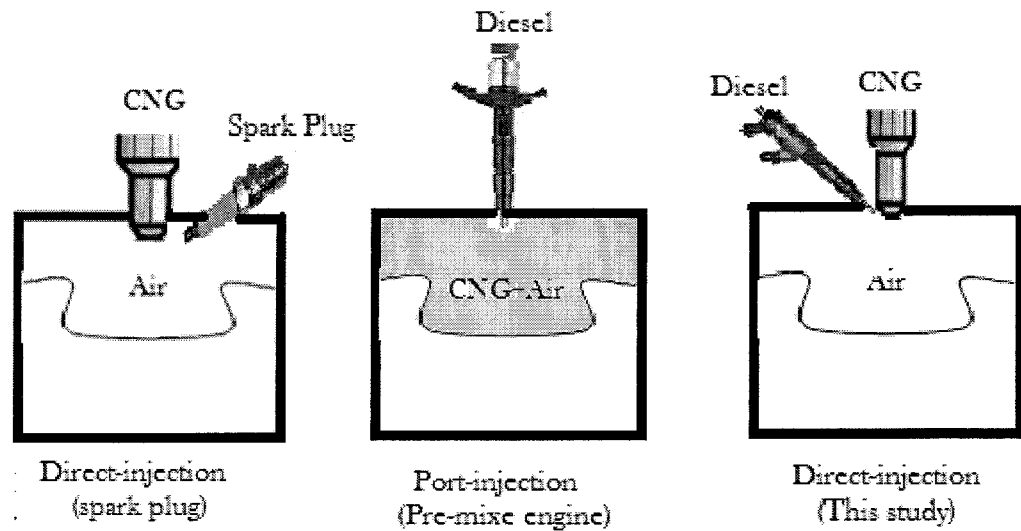


Figure 1.1: Methods of Using Natural Gas in Engines

It appears that direct injection of natural gas with diesel pilot ignition is one of the most promising ways of meeting the energy crises and emissions regulation, analogous to the benefits provided by a common rail high pressure direct injection engine.

However, a more in depth understanding of the interaction between the natural gas jet and the diesel fuel spray and their wall interaction is required in order to realize the full potential of this method.

1.2 Spray characteristics and spray-wall impingement

The fuel spray characteristics, spray-wall impingement and mixture preparation inside the combustion chamber are generally accept as having a powerful effect on the engine performance and the power output [8]. Based on the previous studies the spray characteristics and spray-wall impingement of conventional fuels are largely dependent upon the fuel atomization and evaporation [9, 10], hence, these characteristics play a crucial role in the design process of an internal combustion engine. In addition, these characteristics not only aim to improve the engine efficiency, but also assist the understanding of parameters used to judge fuel spray performance. For example, the spray penetration length must neither be too long nor short in a combustion chamber. If too long, impingement could occur resulting in wetting of cylinder walls and/or piston crown [11]. This would consequently lead to the formation of soot and wastage of fuel. If too short, a reduction in the mixing efficiency and hence good combustion will result.

Studies of the fuel spray characteristics can be classified into two basic categories: macroscopic and microscopic. The first one, which involves spray tip penetration, spray cone-angle, and their derivatives [10, 12] and the second involves droplet velocity, droplet size, size distribution and air fuel ratio [12]. Macroscopic properties of diesel and CNG can be measured by direct visualization methods such as Shadowgraphy and Schlieren technique and analyzed using image processing systems and cheaper laboratory equipment than the ones that microscopic measurements require. Furthermore, macroscopic characteristics of CNG and diesel fuels are more reliable, since they can be easily measured.

1.3 Problem statement

The main disadvantage of compressed natural gas as engine fuel is its low flame propagation speed, narrow combustible range and high ignition energy, therefore the implementation of natural gas (NG) in direct injection compression ignition engines (DICIEs) is difficult because NG does not auto-ignite under compression ignition engine conditions. A possible solution for this problem, is to inject natural gas with diesel fuel (high-cetane number) directly into the combustion chamber [7].

Actually, the development of high performance NGDIEs is unclear as the macroscopic characteristics of the diesel-CNG dual fuel jet which differs considerably from that of diesel fueled compression ignition (CI) and spark ignition (SI) engines. Based on the previous studies, it is well known that the injection strategy and the atomization play an important role for the diesel spray, and the mixture formation is largely dependent upon the droplet distribution and evaporation. In contrast with diesel spray, natural gas does not have droplets and evaporation at all. Therefore, in order to develop better understanding of the direct injection of natural gas combined with diesel fuel, macroscopic characteristics of natural gas jet, diesel spray, and their combination together with presentation of the jet radial travel along the wall were experimentally investigated in this work.

1.4 Scope of the Research

This research is basically focused on the visualization of the gas jet propagation, diesel spray, and their combination together with jets-wall impingement at different injection pressures (Natural gas: 18, 16 and 14 bar and Diesel: 500, 600 and 700bar), wall temperatures (300-500°K) and injector-wall distance (80, 60, 40 mm). The research also involved a design of a test rig with optical access from two directions.

Macroscopic parameters such as spray tip penetration, spray cone angle, spray velocity, spray impingement (spray travel along the wall : radial penetration and spray height) of CNG, diesel and diesel-CNG dual-fuel jets were recorded with a high speed camera using the Schlieren imaging technique and associated image processing software (MATLAB).

1.5 Research Objective

The main objectives of this work are

- To investigate the jet characteristics of CNG and jet-wall impingement at different injection pressures and injector-wall distance.
- To investigate the spray characteristics of the diesel and diesel-CNG dual-fuel jet and jet-wall impingement at different injection pressures, injector to the wall distance and temperatures.
- To study the effect of the CNG jet on the diesel spray characteristics and wall interaction at the same conditions.

1.6 Outline of the Thesis

This thesis is divided into five chapters. Chapter 1 introduces the background of depletion of fossil fuels, the air pollution caused by conventional liquid fuel and renewable clean burn alternative fuels. It also describes developments in the use of natural gas in engines, and provides preliminary indications of the potential benefits of natural gas fuel, the importance of spray characteristics and its wall interaction in internal combustion engines. In addition, the chapter illustrates the research problem, objectives and scope of work.

Chapter 2 highlights the ground works related to the application of CNG and diesel-CNG dual fuel in direct injection and compression ignition engines. It also discusses the spray characteristics and spray-wall impingement of CNG and diesel fuels, and presents the earlier research investigation of natural gas jets and diesel spray relevant to the present study.

Chapter 3 describes the detailed methodology of the experimental work which includes experimental setup, test rig design, gas supply systems, diesel injection system, test calibration, data acquisition and triggering, Schlieren visualization system and the image processing technique.

Chapter 4 presents the results and discussion of the study. The experimental results are presented in graphical forms which elaborate the results in detail.

Finally, Chapter 5, which is the last chapter, shows the major conclusion and recommendations for future work.

CHAPTER 2

LITERATURE SURVEY

2.1 Compressed Natural Gas as an Engine Fuel

The rapid depletion of the world oil reserves, high cost of oil refining, and the harmful effects of air pollution linked to vehicular usage have led researchers and designers over the world to carry out research in solving the problems. There is a great effort in industry and engine research centers to propose alternative fuels for the usage in internal combustion engines. Alternative fuels are any materials or substances that can be used as fuels, other than conventional fuels (diesel and gasoline). Some of these fuels are emitting less air pollutants and they are very economical compared to conventional fuels [13].

Currently, natural gas is regarded as a promising alternative fuel in order to solve both problems of the energy crisis and emission regulation. Natural gas can be compressed; therefore it can be stored and used as compressed natural gas (CNG). Most of the research interest is focused on the use of CNG as an alternative fuel, mainly due to its wide availability in nature with low cost compared to other alternative fuels. CNG as fuel is regarded as one of the most promising alternative fuels because CNG has high octane number which allows the engine to be operated at higher compression ratio and hence yielding higher thermal efficiency. CNG has a low carbon/hydrogen ratio, meaning that it produces less hydrocarbon per unit of energy realized [2, 14].

Despite the advantages of CNG as one of the most important alternative fuels, there are many problems facing the use of CNG as fuel in internal combustion engines because CNG has a low cetane rating and is not suitable for compression ignition due to the high ignition temperature and losses in volumetric efficiency [13, 15]. The

lower performance of engine combustion is basically caused by two main factors: CNG fuel characteristics and the improper operation condition of the CNG engine. Over the past decades, CNG has been tested as an engine fuel for different internal combustion engines. The main types include the premixed charge spark ignition engine, the lean burn engine, the dual fuel-pilot injection engine and the direct injection engine [2-5].

2.2 Compressed Natural Gas in Spark Ignition Engine

The vast majority of natural gas engines are premixed charge Spark Ignition (SI) engines. SI natural gas engine has been widely used in internal combustion engine and it has shown significant advantages over diesel and gasoline engines in term of emissions [2, 5, 16-17]. Jahirul et al. Investigated the engine operation with CNG and compared with gasoline in full load condition. The following findings had been obtained: the volumetric efficiency reduction by (10-14.4%), the torque and power output reduction by (10.8-14%), while the thermal efficiency of CNG fuelled engine increased by (22 and 33%) and the emissions of CO and CO₂ decreased. Premixed SI engine suffers 30% lower power output than equivalence size diesel engine due to knocking limitations [16]. In addition, SI engines suffer high pumping losses, due to the need to throttle the intake air at part load conditions which leads to the reduction in volumetric efficiency. For these reasons, many researchers have been proposing the addition of a secondary fuel to the pure CNG in order to enhance combustion performance.

The concept of using natural gas in dual-fuel engines (CIEs) is not new. This technology combines the clean and flexible combustion attributes of natural gas with the easily ignitable diesel fuel in order to obtain a high degree of diesel fuel replacement [18, 19]. There are two main methods on how to use natural gas in dual fuel engines: pre-mixed and direct-injection. The first one, the primary fuel (natural gas) is induced into the cylinder and mixed with air before the compression stroke. A mixture of gas and air is compressed and before the end of the stroke, a pilot quantity of diesel fuel (depending on the operating conditions) is injected to initiate combustion. The processes involved in dual-fuel engines lay between that of the

compression ignition (CI) and SI engines. This type of operation has advantages in reducing the emissions and increase the thermal efficiency [20]. On the other hands, it has a drawback namely possessing lower power output in a high engine load, this due to the engine suffering from knocking resulted from combustion of premixed natural gas and air [21].

The superior efficiency of the direct injection compression ignition engines (DICIEs) can be traced to two major factors: possess high compression ratio and does not require air throttling to operate under part load operation [5]. To analogize with these benefits provided by DICIEs, the direct injection of natural gas in compression ignition engines is considered to be the final target.

2.2.1 Compressed Natural Gas in DICIEs

Direct injection approach seeks to satisfy the desire to achieve Diesel cycle operation using natural gas as the fuel. Recently, the usage of direct injection of diesel-CNG dual fuel system has been developed and its capability has been demonstrated for the usage in diesel pilot-ignited high pressure direct injection system. This system uses a small diesel pilot-injection in order to provide an ignition source and a late cycle direct injection of natural gas. The system also allows diesel cycle operation with over 90% replacement of diesel fuel [22, 23]. The concept eliminates both part-load throttling and limits on torque due to the onset of knock.

Douville et al. [24] used a two stroke engine to compare an early direct injection natural gas system with diesel engine. In case of the natural gas engine, both CO and NO_x emissions were reduced by 15-20% and 20-40% respectively, while the particle matter (PM) emissions were almost unchanged. On the other hand, the thermal efficiency were almost identical at medium and low load but were higher for NG fuelling at maximum loads. The methane emissions were higher at low loads but can be lowered with system refinement.

High pressure direct injection engines seem to be one of the most efficient ways to tackle stringent emissions while enhancing the thermal efficiency of engines. The use of high pressure common rail systems in recent years has become a very attractive

way to illustrate the efficiency [9]. High pressure injection seems to induce a very different spray characteristics structures than that of earlier low pressure sprays. Using high pressure direct injection of diesel pilot and natural gas as effective fuelling method has been confirmed by Munshi et al. [25]. Their results have shown that when small quantity of diesel were injected with a direct injection pressure of natural gas, diesel-like thermal efficiencies were achieved while substantially reducing of PM, NOx and CO emissions were noticed.

The improvement in direct injection natural gas dual fuel engines can be obtained by varying their injection pressures (natural gas and diesel pilot). For compression ignition engines (diesel engine), increasing the fuel injection pressure improves fuel atomization, evaporation as well as mixture formation inside the combustion chamber [26, 27]. A similar effect occurs in direct injection of the natural gas in the dual fuel engines. ~~Increasing the injection pressure of diesel pilot fuel from 200 bar to 600 bar,~~ resulted in an increase in combustion chamber pressure by about 30% at 40 ms after the injection. The higher injection pressure gave a faster combustion of the natural gas, resulting in an increase in performance of dual fuel combustion [19]. Another study by Brown et al. [23], used a single cylinder research engine to investigate the direct injection of natural gas and diesel fuel using co-injector under different conditions in terms of knock and emissions.

From the previous studies, it is clear that the performance of dual-fuel (diesel-CNG) direct injection engines is influenced significantly by two factors: the diesel spray (pilot-ignition for durability and ignition quality) and the CNG jet propagation. But those factors are largely dependent upon the injector's structure and injection strategy such as fuel spray characteristics which is playing an important role in the mixing processes inside the engine. The spray characteristics such as spray penetration rate, spray cone angle, spray velocity, droplet size and droplet atomization are largely dependent upon the injection pressure, chamber pressure and temperature [12, 28].

Furthermore, the CNG jet propagation is very important because it determines the quality of combustion which is completely different than that of diesel spray, for example: there are no liquid sheets, droplets and evaporation at all with low jet

momentum [18]. Hence, understanding of the diesel-pilot spray characteristics as well as spray-wall impingement together with CNG jet propagation in dual-fuel injection are essential and are the central goal for the diesel-CNG dual-fuel direct injection improvement.

2.3 Diesel Spray Characteristics and Spray-Wall Impingement

A detailed understanding of the fuel injection, spray characteristics, spray-wall impingement and the mixing processes of the diesel-CNG dual fuel injection engines is required in order to enhance the combustion within engine cylinders, while not compromising the engine fuel economy. In recent years, comprehensive research studies have been carried out in the field of diesel injection and diesel spray characteristics [9, 12, 26, 29-31]. Based on the previous studies, the fuel spray characteristics can be classified into two basic categories namely macroscopic and microscopic. The former involves spray tip penetration, spray cone-angle, and the derivatives of them such as spray tip velocity and spray volume; and the latter involves droplet size, droplet distribution and air fuel ratio distribution.

Macroscopic properties of liquid sprays and gaseous jets can be measured with direct-visualization technique and using image processing software for analysis, which is a cheaper laboratory tool than the ones that microscopic properties require. In addition, macroscopic characterization is more reliable since there larger in dimensions and easily detectable.

Direct-visualization techniques such as photography, shadowgraphy and Schlieren are common ways being used in the optical research. Direct photography is the least complicated technique but only the liquid and flame propagation can be recorded. Back illumination photography uses a diffused light source which is located behind the target. This type of photography produces a dark object with a bright background. Shadowgraphy produces similar output as the back photography where the target is back illuminated and a dark object shadow is recorded on a bright background [31]. Schlieren photography technique is the most commonly used for qualitative investigations such as gaseous fuels and vapor fuel spray [32].

The dependence of the spray penetration on injection pressure and the ambient pressure differed significantly from one study to other. Kennaird et al. [26] used a Schlieren technique to quantify both liquid and vapour distribution of a diesel fuel injected through a single and multi-hole nozzles using a modern common rail fuel injection system. The diesel spray images were processed using digital imaging program. The authors concluded that the penetration rate from each hole was the same for single and multi-hole nozzles once the nozzle was fully open. An increase in the penetration rate was observed at higher injection pressures and lower gas densities.

Ghurri et al. [33] visualized diesel and biodiesel blends injected through a common rail injection system to qualify and quantify their macroscopic characteristics. The spray images showed that the spray tip penetration of diesel fuel was slightly higher than that of biodiesel blends. At low injection pressure, they were almost the same. ~~Both fuels were relatively similar for the same spray cone angle.~~ The spray tip velocity increased at the start of injection and it decreased after reaching the maximum value.

Taşkiran and Ergeneman [10] designed a constant volume chamber which was heated up to 825 K at 35 bar to visualize the diesel spray characteristics injected from different nozzle geometries. Their results showed that the spray tip penetration became longer as the injection pressure increased, while it shortened when the ambient pressure and temperature increased. It was also noticed that both spray cone-angle and spray tip velocity were higher at the initial regions and became lower after the spray developed.

An investigation on the effect of injection pressure of diesel, biodiesel and jet fuel under non evaporating conditions through a common rail system on the microscopic spray characteristics was visualized by [30]. Their images showed that the spray tip penetration increased as injection pressure increased. Biodiesel showed longer penetration beyond others at low injection pressure but their differences became small at higher injection pressures. On the other hand, the spray cone angle was influenced by the injection pressure; the cone angle converged to its steady state as the injection pressure was increased. The authors also evaluated the spray volume by combining

the data of spray tip penetration and cone angle, and it was noticed that larger spray volume could be observed under high injection pressure.

The macroscopic spray characteristics of diesel and liquefied petroleum gas under different injection and ambient pressures were investigated numerically and experimentally by [34]. The spray tip penetration derived from images showed that diesel was the longest among others. The authors also noticed the effect of ambient pressure on spray tip penetration: as ambient pressure increased, spray tip penetration decreased.

De Risi, et al. [35] Investigated macroscopic characteristics of diesel sprays injected through electronically controlled common rail single-hole injector in the 300 K, 623 K, 1085K temperature ranges corresponding respectively to 1, 6 and 12 bar ambient pressures using measurement systems based on a high-speed digital camera. They found that the spray tip penetration and spray cone angle reduced proportionally with the temperature.

The effect of injection duration and the injection pressure on macroscopic spray characteristics were studied by [36]. Their results showed that the spray tip penetration increased proportionally with the injection duration and pressure, and the spray diluted at the end of injection. They also noticed that as ambient temperature increased the spray tip penetration decreased. On the other hand, the spray cone angle was enhanced with higher ambient pressures.

2.4 Natural Gas Jet Characteristics and Jet-Wall Impingement

In the past decades, most of the research studies focused on the liquid fuel atomization and realised great achievements. Based on their results, it was well known that the injection characteristics and injector structure played an important role in the liquid fuel spray characteristics such as spray penetration and spray cone angle. In contrast to the liquid fuel spray, the gas jet propagation does not have droplets and evaporation at all with low jet momentum [32]. On the other hand, the CNG injector should be fully different from the diesel injector due to the tremendous difference between gas and liquid physical properties.

Despite the differences, many studies have been carried out on the high pressure natural gas jet characteristics using different optical methods. For example, gas jet characteristics at injection pressures of 50 to 80 bar in a constant volume chamber was visualized using planar laser-induced fluorescence (PILF) technique were investigated by [37]. Their results showed that the gas jet was generally narrow with cone angle: 23 degree and the maximum width of 25 mm. The jet penetration length was 90-100 mm at fully developed gas jet propagation. The authors concluded that the penetration length was proportional to the square root of elapsed time, and inversely proportional to the ambient pressure.

High injection pressures of the gas require high performance injectors which are associated with high energy consumption to produce them. From this point of view, low pressure gas jets are considered to be a new target.

One of the most recent experimental studies was by Mohammed and Iffa [38] Who studied the gas jet characteristics of the CNG and H₂ under atmospheric pressure and temperature. The authors used a low injection pressure gas injector (1.2 MPa to 1.8 MPa) and Schlieren photography technique for the jet visualization. The jet images were analyzed using an image processing system which measured the penetration and cone angle. Their results showed that, with an increase in the injection pressure, both penetration length and cone angle increased.

Liu et al. [14] investigated the compressed natural gas jet development processes under different injection pressures (1, 3, and 5 MPa) using the Schlieren photography technique. They found out that the CNG spray penetrated axially and radially at the start of injection, and as the injection continued, both tip penetration and cone angle increased. The initial spray angle under higher injection pressure was smaller, but it increased faster (approximately 2ms after the start of injection).

Natural gas jet/wall impingement is considered as a promising way to control and enhance the mixing processes in the combustion chamber.

Senoo et al. [39] investigated the wall impingement of natural gas jet at high injection pressure using direct-visualization images in a constant volume vessel under different ambient conditions. The authors showed that the jet impingement was

affected by the distance between the injector nozzle and the wall as well as the injection pressure. Yu et al. [40] studied the wall-impinging gas jets and mixture formations under low pressure (e.g. 3 and 7 bar) using the PLIF technique. Their results showed that the interaction between the gas jet, wall impingement and surrounding air had a good effect on the mixing process. A high injection pressure led to higher mixing efficiency. The authors concluded that the low-pressure jet wall-impingement was considered a promising approach to enhance the mixing process.

2.5 CNG Jet and diesel spray dual injection Characteristics and Jet-Wall

Impingement

The technology of using gas-assisted atomization of liquid fuel was considered to be the final target for using CNG in CIEs. In the previous work, Chepakovich [18] used co-injector to assist diesel atomization in a pre-chamber. Their study was focused on the effect of gas to the chamber pressure ratio in a diesel engine. Their main results have shown that the penetration of the gas and gas-diesel jets depended strongly on the pressure ratio, while the chamber pressure was not significant. Yang [41] used a separate mixing chamber to assist the diesel atomization by a gas injection. In their system, low injection pressures were used. In a more recent study in this area, Birger [7] used co-injector to study the gas (high pressure) assisted atomization of the diesel spray in an optical constant volume chamber. The jets were visualized using a high speed camera while the images were processed using the MATLAB software. The authors compared the images of two-phase co-injector jets and the pure diesel injection jets. They noticed that the co-injector was better for diesel atomization. However, when the co-injector was operated at high injection pressure, low gas flow rate per quantity of diesel injected was observed.

2.6 Summary

The previous researchers advocated that using the CNG in DICIEs was the best option to supplement diesel engine operation. In the past few decades, most of the researchers focused on the visualization of the diesel and diesel blends spray

characteristics, while others visualized the natural gas jet propagation. It is well known from the previous studies that the macroscopic characteristics such as: spray tip penetration, spray cone angle and their derivatives together with the spray wall-impingement play an important role in the mixture formation inside the engine. In addition, a few workers built their chambers to visualize the diesel-CNG dual-fuel using co-injector (high injection pressure). However, the co-injector needs too much energy consumption with high injection pressure. In addition, the mixing process of the dual-fuel needs high gas pressure to be supplied by a high energy-compressor. Also, with a high injection pressure, low gas flow rate per quantity of injected diesel will be produced.

It is therefore concluded that there are potentials for further improvement of the atomization characteristics of the dual-fuel direct-injection, using a low injection pressure of CNG jets assisted by high injection pressure of diesel spray. This method might be the preferred one for the future direct-injection engines.

The present work investigates the propagation of CNG jets, a diesel spray and their combination created by CNG and diesel electronic injectors. This is done with the aid of flow visualization. The results of this work suggest that using two parallel injectors (diesel injector associated with low gas injector) system is expected to improve the macroscopic characteristics of the dual-fuel direct injection.

CHAPTER 3

EXPERIMENTAL WORK

This chapter describes the special experimental test rig design and the procedure for image acquisition used in the present work. Visualization of the CNG jet, diesel spray, and their combinations (diesel-CNG) has been done using two electronic injectors (CNG and diesel) and with a Schlieren system for flow visualization. The image acquisition was made by using a high speed video camera (Phorton, FASTCAM-APX). A computer software package based on MATLAB was built and used for the image processing and the calculation of the quantitative data.

3.1 The Experimental Setup

There were three major objectives in setting up the experimental rig, to capture the fuel spray in a constant-volume chamber as far as the fuel supply, injection duration, injectors-wall distance and injection pressures are concerned. This allowed the use of two injectors (diesel and CNG) as those (co-injectors) which are employed in the performance testing in the engines. The rig was also developed to facilitate the use of the Schlieren technique, as well as using a light-source to be able to visualize the gas jet propagation and to satisfy the requirements of safety, reliability, and ease of operation.

3.1.1 Test Rig Design

Generally, Spray research has been performed in a number of different test rigs: special research engines, high pressure and high temperature bombs, flow rigs and constant volume chambers. A constant volume test rig was considered as the best option for fundamental research as it combined good optical access, large observation

areas and good control of scavenging before injection. A chamber, 100 mm high and 86 mm wide (similar to the stroke & bore of a CNG engine in the UTP automotive lab), was designed and built to allow for optical analysis of both the jets and wall impingement as shown in Figure 3.1. The bottom plate of the test rig was made from aluminum (piston material) with a k-type thermocouple inserted in it for temperature measurement.

From previous work [7] the author noticed that, after about 10 injections, it was difficult to see the subsequent injection (the diesel spray droplets contaminated the windows which obscured the view). To avoid this problem, the optical access into the chamber was provided by two removable glass windows, shown in Figure 3.1, giving an optical access 76 mm wide and 80 mm high. The design was optimized to allow visualization of the gas and liquid propagation using the Schlieren technique. The glass plates were easily removable for cleaning or replacement.

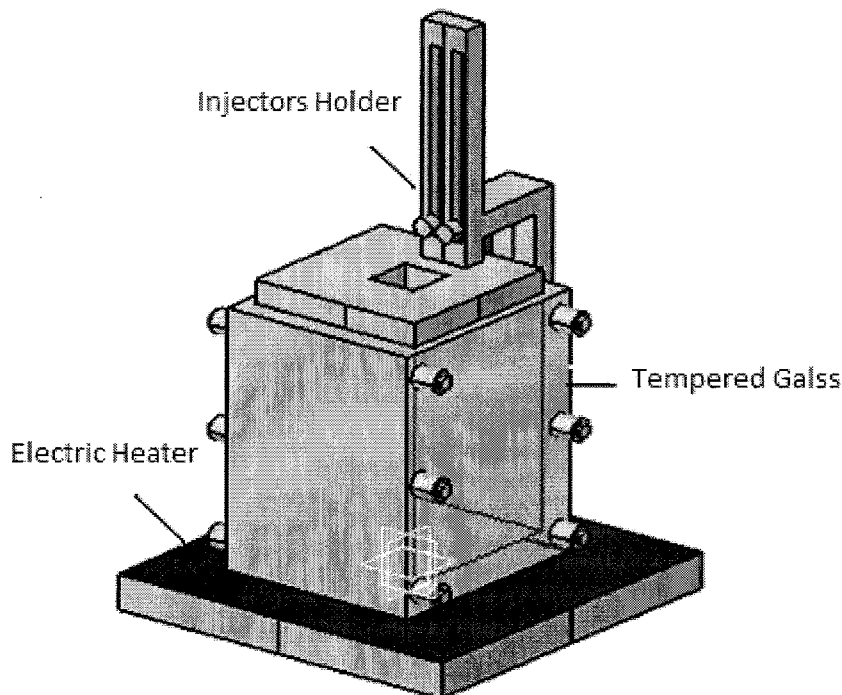


Figure 3.1: Experimental Test Rig

Different methods were used in previous studies for achieving representative temperature conditions in the rig e.g. some used direct heating of the walls (bottom) of the test rig [42], while others used an electric heater [19] inside the plate. In this

study, a controlled electric heater was used to heat the bottom plate. In previous studies, different researchers measured the temperature variation inside engines [43, 44]. In this study, the choices of the wall temperature was based on the pervious study [44], who used thermocouples to measure the temperature variation at different piston points and different diesel engine operating conditions. The maximum temperature recorded in the piston head was reached at a near-full-load engine condition. A holder of the diesel and CNG injectors was mounted in the center of the test rig's top plate (both of them adjusted to be in the axial direction) which was moved up and down to vary the injector-wall distance in the range 80-40mm. The experimental test conditions are given in table 3.1.

3.1.2 CNG Injection System

Fig. 3.2 shows a schematic diagram of the CNG injection system which consisted of a CNG cylinder (the pressure inside the cylinder was up to 200 bar), two pressure regulators (double stage), CNG pressure gauge, a pressure regulating valve, and a solenoid-type CNG injector with a maximum pressure of 20 bar as shown in Fig 3.3. A National Instrument deriver and a power supply (12V) were used to drive the injector through a program built on Lab View version software to control the injection duration.

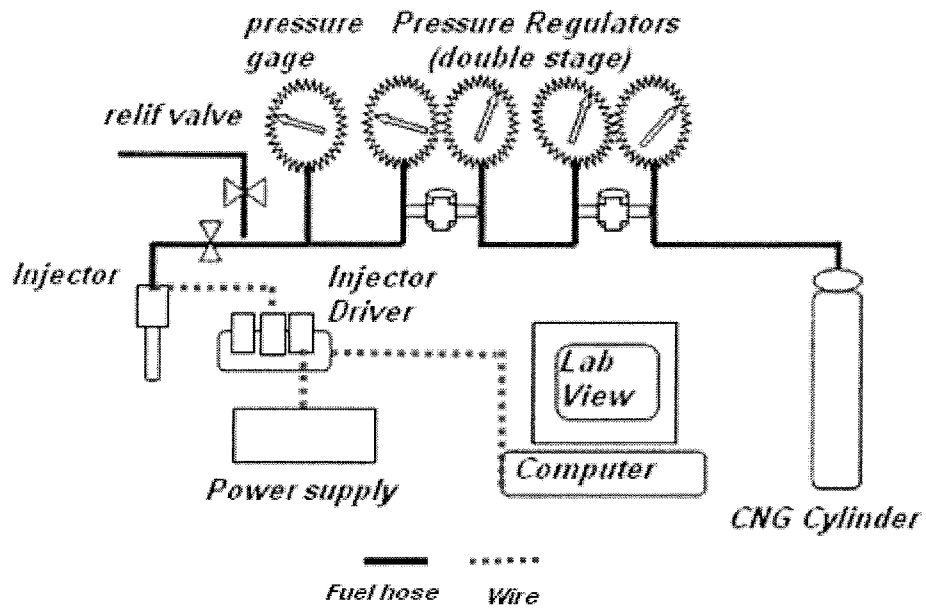


Figure 3.2: CNG Fuel Injection System.

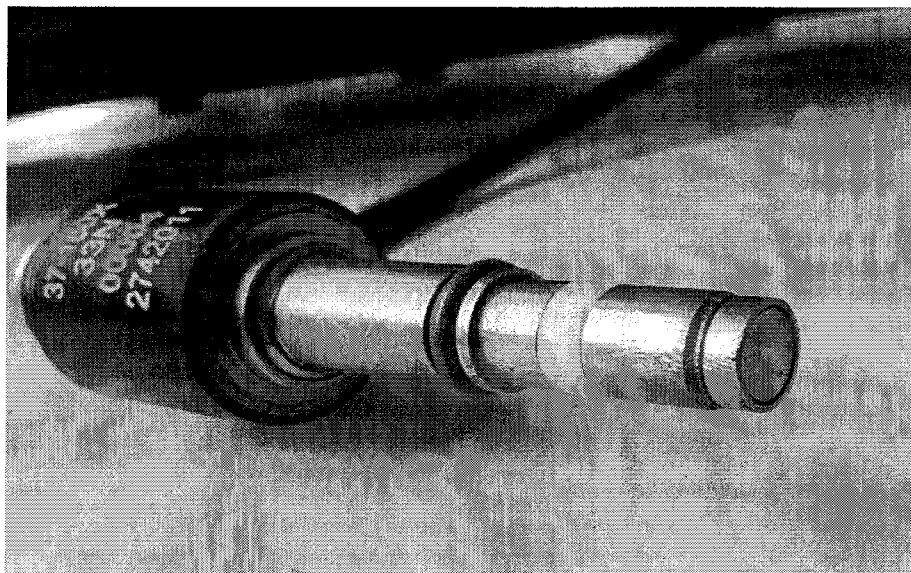


Figure 3.3: Natural gas injector

3.1.2.1 CNG Composition and Properties

Compressed natural gas supplied by Gas Malaysia Snd. Bhd. was used in the study of the jet characteristics and propagation. The specifications of the CNG are given in Table 3.2 and the properties are in Table 3.3.

Table 3.1: Experimental condition

FUEL	CNG	DIESEL
Injection pressure (bar)	14, 16 and 18	500, 600 and 700
Injection duration (ms)	5	5
Ambient pressure (bar)	1	1
Injector wall distance (mm)	80, 60 and 40	80, 60 and 40
Wall temperature (K)	300, 400, 500	300, 400, 500

3.1.2.2 CNG Injection Measurement

The positive displacement method described by [45] was used to calibrate the gas flow meter. This required a simple setup and a laboratory procedure. The gas flow was sent to a reservoir with rigid walls and full of water. As gas entered the reservoir, the water flowed out and the amount of water exiting the reservoir in a given time interval could be collected with the container in the same time interval, the mass flow rate of water leaving the reservoir was equal to the gas volume flow rate entering it (The volume was calculated with the density to be unity). This was considered to measure the volume of CNG as shown in Figure 3.4. Their mass flow rate versus injection duration with different injection pressures are shown in Fig. 3.5.

Table 3.2: Typical Composition of the CNG in Malaysia [16]

COMPONENT	SYMBOL	VOLUMETRIC%
Methane	CH ₄	94.42
Ethane	C ₂ H ₆	2.29
Propane	C ₃ H ₈	0.03
Butane	C ₄ H ₁₀	0.25
Nitrogen	N ₂	0.44
Carbon dioxide	CO ₂	0.57
Others	H ₂ O+	2.00

Table 3.3: Fuel Properties of CNG [46]

FDUEL PROPERTIES	NATURAL GAS
Density at 1 atm, at 300 K (kg/m ³)	0.754
Stoichiometric air to fuel ratio (vol%)	9.396
Stoichiometric air to fuel ratio (wt%)	0.062
Laminar flame speed (m/s)	0.380
Quenching distance (mm)	1.900
Mass lower heating value (MJ/kg)	43.726
Volumetric heating value (MJ/Nm ³)	32.970
Octane number	120
C/H ratio	0.251

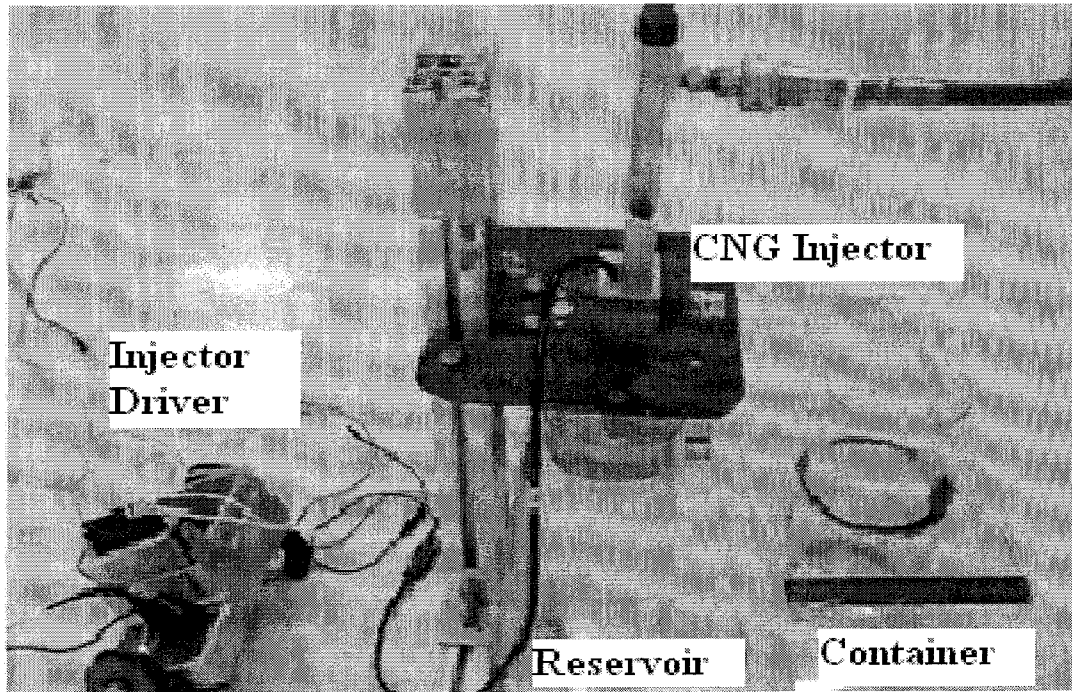


Figure 3.4: The set up for the injector flow calibration

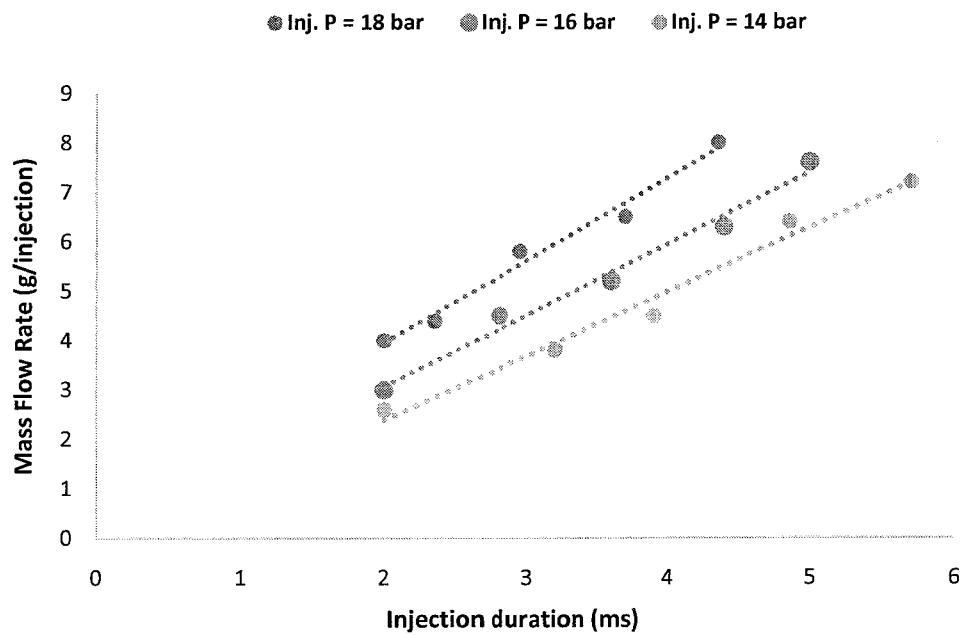


Figure 3.5: Mass Flow rate versus injection duration for different injection pressures

In order to get the mass flow rate from the injection duration for different injection pressures (i.e. 18 bar, 16 bar and 14 bar) the following cured equations were used:

$$m = 1.6639x + 0.6265 \quad \text{for 18 bar,} \quad (3.1)$$

$$m = 1.4406x + .1914 \quad \text{for 16 bar,} \quad (3.2)$$

$$m = 1.298x - 0.2052 \quad \text{for 14 bar.} \quad (3.3)$$

Where m = mass flow rate and x = injection duration.

3.1.3 Diesel Injection System

A common rail, electronically controlled injection system was used to generate and induce the high injection pressure sprays into the chamber. This injection system provided flexibility in controlling the injection timing, injection duration and the rail pressure. The fuel injection equipment included: an electric motor, a control unit, a high pressure fuel pump, a high pressure delivery pipe, a common rail, a regulator valve, a pressure gage, an injector and an injector driver.

The fuel injector used was a modern electro-magnetic actuated common rail injector as shown in Fig. 3.7. In order to study a single fuel spray, different researchers modified their injectors from different numbers of holes to study a single-hole nozzle. Kennaird et al. [26] in their study of multi-hole and single hole injectors sprays penetration characteristics found that, the single-hole injector was valid to characterize the spray. Therefore, the injector used in this study was modified from 6 to a single-hole (0.3 mm diameter) to characterize the axial spray penetration.

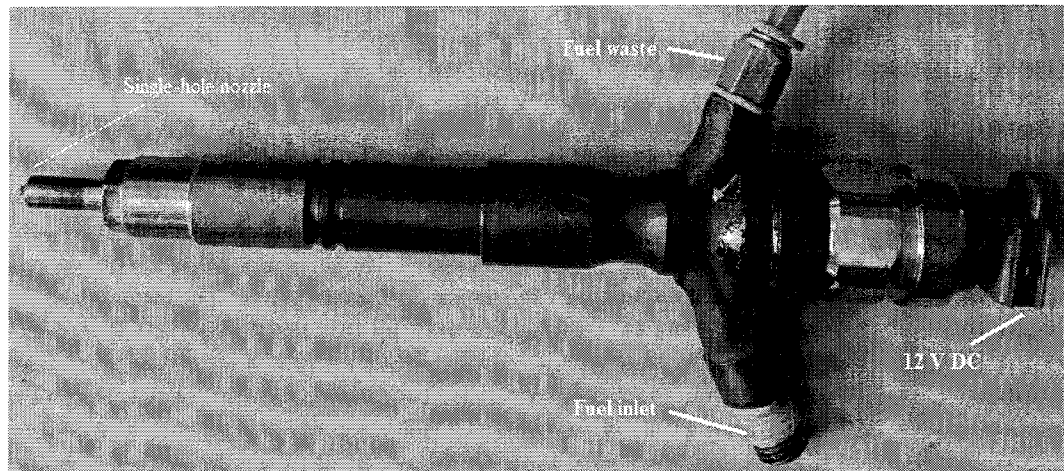


Figure 3.6: Common rail injector used for diesel spray study.

The fuel pump (high pressure) was powered by an electric motor (2 horsepower with a maximum the speed of 1420 rev/min) through timing belt pulleys. The AC motor was controlled by an electronic control unit (ECU). To ensure stable set rail pressure, a pressure regulator valve and pressure gauge were used. An injector driver circuit was built and used to control the opening and closing of the injector valve by which we were able to control the injection timing and injection duration which was built in a lab VIEW program. Figure 3.7 shows a schematic of the connections between these components.

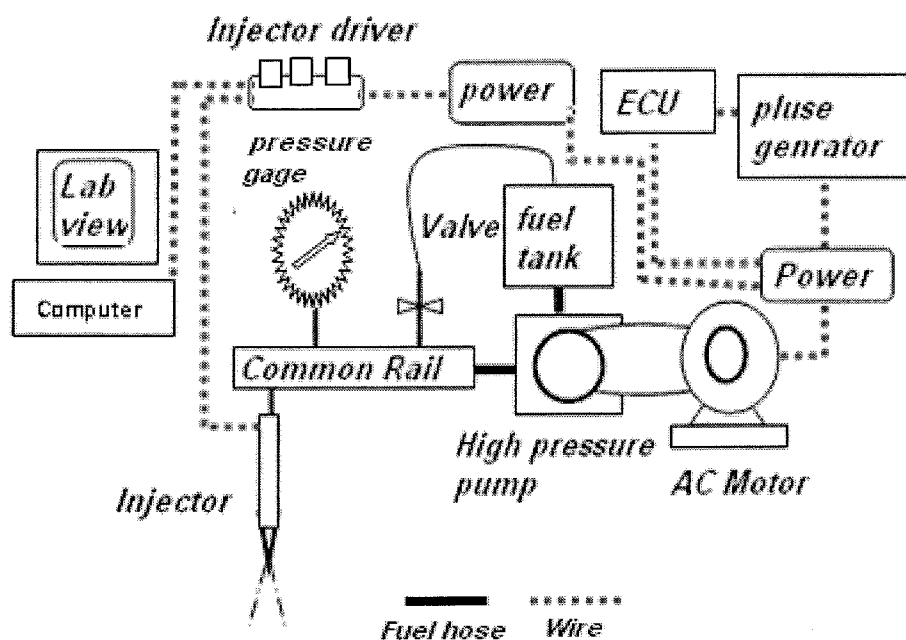


Figure 3.7: Diesel Fuel Injection System

3.1.3.1 Diesel Injection Measurement

The quantity diesel fuel emerging from a single hole injector was calculated based on the pressure difference between the fuel supplied pressure and the ambient pressure in the chamber. As the injected fuel quantity per unit time is a linear function of pressure [47], a quantitative estimate of a single fuel injection as given by Eq. 3-1.

$$Q = \frac{A}{a\rho} \int_{t_o}^t P dt$$

(3.4)

Where: Q is the injected fuel (g/s),

P = injection pressure (bar),

A = cross sectional area of the nozzle in (m²)

a = is velocity of sound in the fuel (m/s),

ρ = density of the fuel (kg/m³),

t_o = time at start of injection (ms) and

t = time at the end of injection (ms).

In this study, the mass measurements were carried out at 500, 600 and 700 bar injection pressures with 5 ms injection duration. The measured fuel quantity against time from the start of injection is shown in Fig. 3.8. The tested fuel was a conventional diesel fuel supplied by Malaysian Petroleum Company (PETRONAS) [48]. Its properties are given in table 3.4.

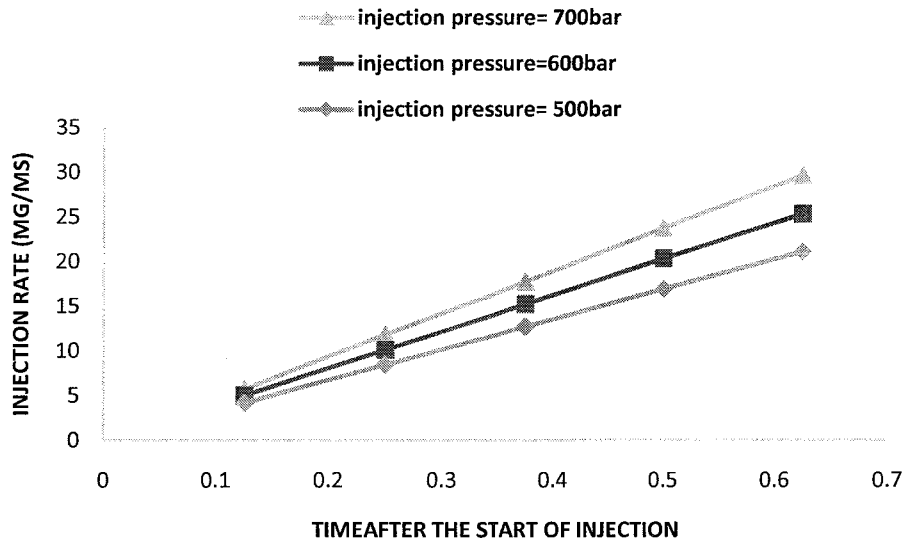


Figure 3.8: Effect of injection pressure on time-resolved injection rate (energizing time of the solenoid is 5ms).

Table 3.4: Properties of Diesel Fuel tested

FUEL PROPERTIES	SPECIFICATION
Density - 15°C (g/cm ³)	0.827
Viscosity - 40°C (mm ² /s)	4.15
Flash point- °C	>140
Calorific value MJ/ kg	42.5

3.1.4 Control System, Data acquisition, and Triggering

The injection control system is shown in Figure 3.9, all fuels and the test rig supply parameters were manually controlled by the use of hand valves and pressure regulators. The injector pulse parameters were controlled by a computer running on National Instruments Lab View software Version. This software was written to allow the synchronization of both injectors (diesel and CNG) with different injection durations. The PID loop program is illustrated in Fig. 3.10.

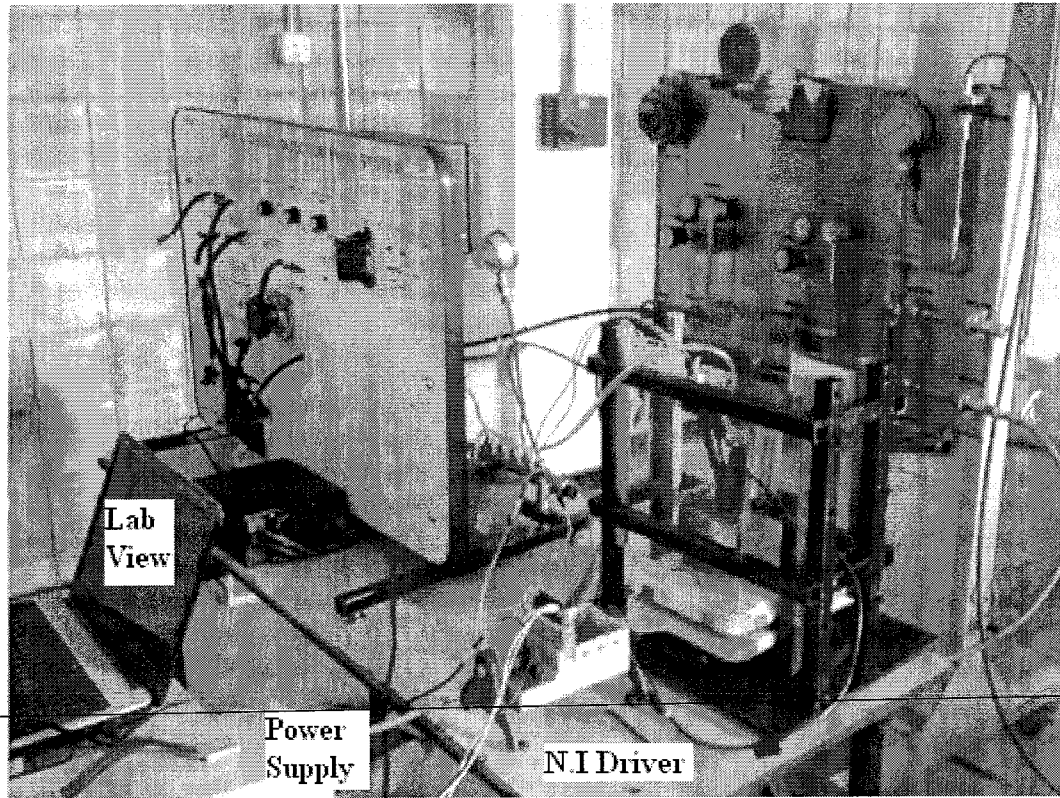


Figure 3.9: Injection control system

The Lab View then output this onto a National Instruments driver Model (NI cDAQ-9174) which in turn generated pulses as specified (boosts the current and voltages of signal), finally sent it to the injectors. A high speed camera (Phorton, FASTCAM-APX) was connected to the computer for capturing and recording through the trigger. As soon as the trigger for capturing started, it was followed by the injection trigger, and the signals sent to both injectors. This allowed us to capture the shape of the jet emerging from the nozzles.

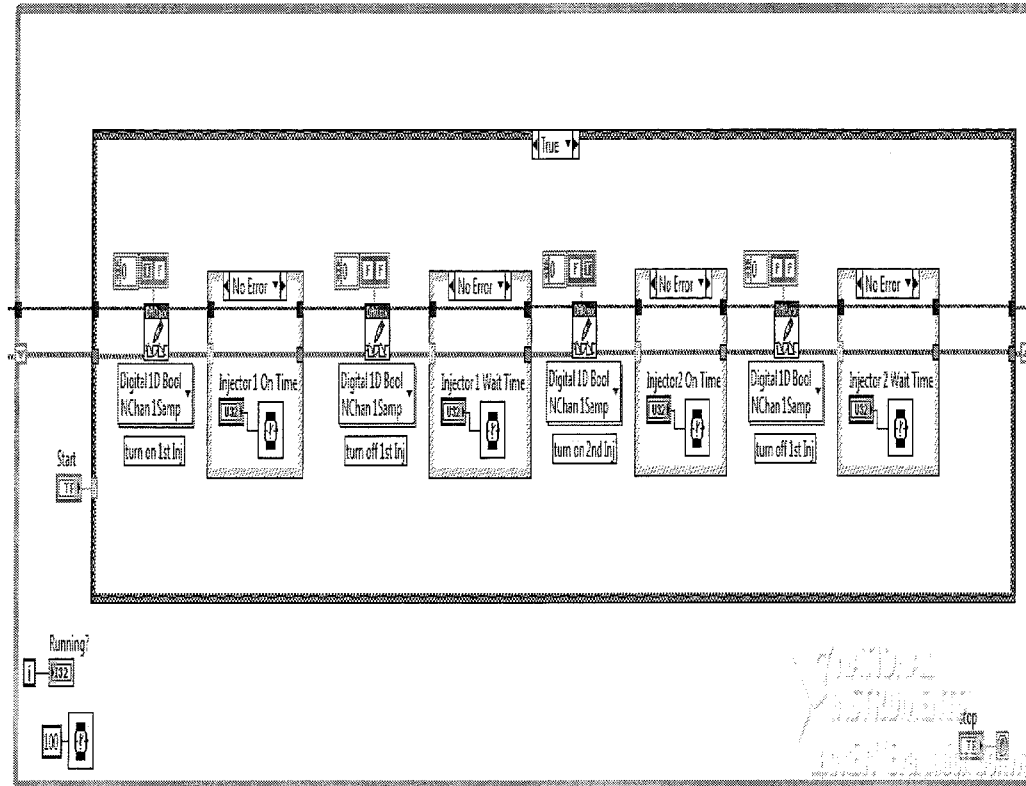


Figure 3.10: Lab VIEW PID loop interface and block diagram

3.1.5 Schlieren Technique

Figure 3.11 shows the general arrangement of the Schlieren system used for flow visualization in the present work. It consisted of a light source, two concave mirrors, a Knife edge, and a high speed camera.

The Schlieren method of flow visualization is based on the phenomenon of deflection of a parallel beam of light passing through a region having a gradient of reflective index in the direction perpendicular to the direction of the beam. To create a parallel beam of light and later focus it onto the camera, two concave mirrors were used. The light source was placed at the focal point of one transmitting mirror and the knife edge was placed at that of the collecting mirror. The light source, the two concave mirrors, and the camera were assembled in a Z-configuration where the two mirrors were positioned at opposite sides and at the same angles to the parallel beam of light. The knife-edge was setup to crop some of the light at the focal plane,

the whole image darkened uniformly and the density gradients became observable as scales of grey (the light let past the knife-edge will be affected by density changes, and interference with the rest of the disturbed light will be prevented by inserting the knife-edge) [49].

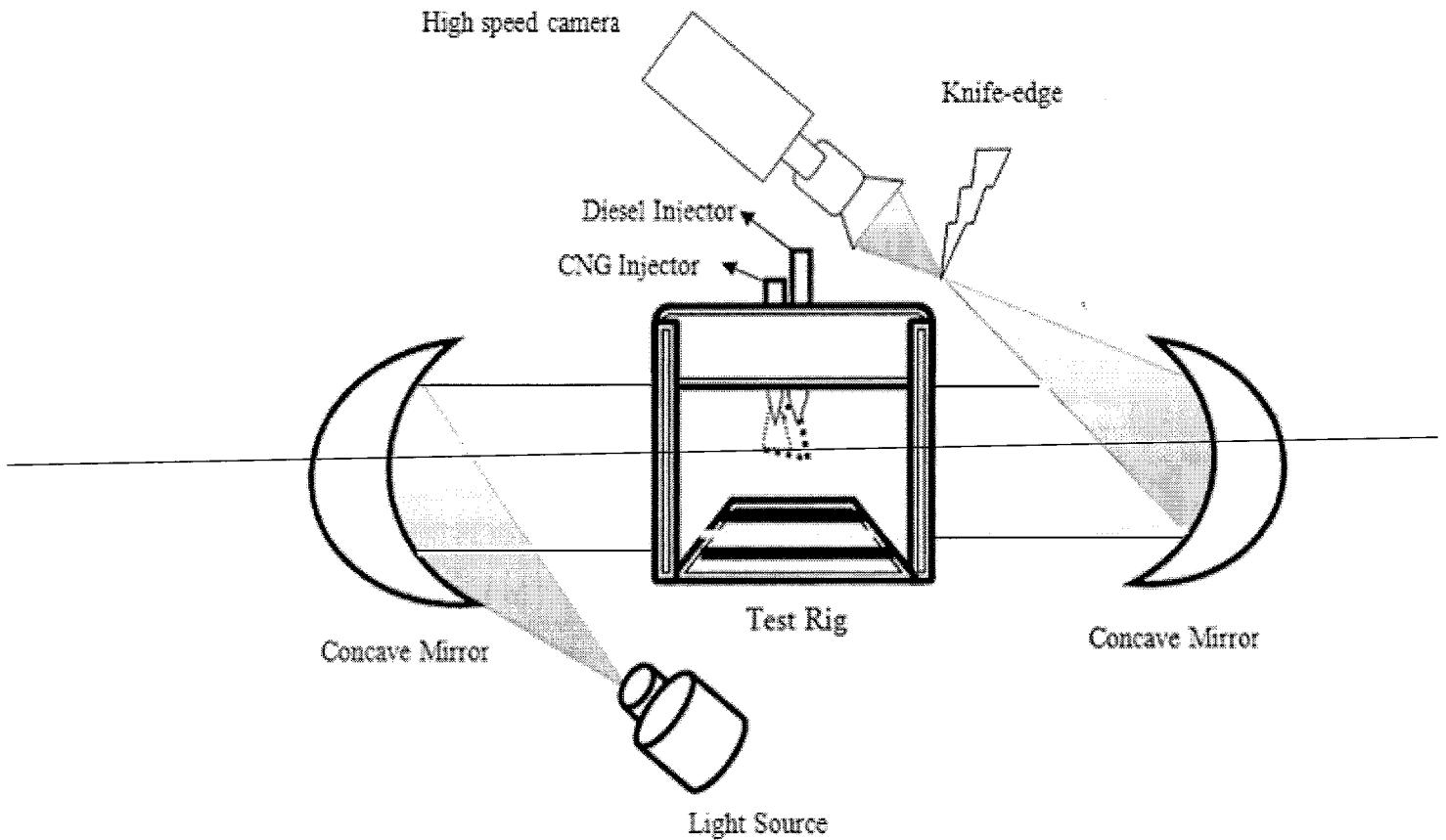


Figure 3.11: Experimental set-up for Schlieren technique.

3.1.6 Image Processing

A high speed video camera (Photron, FASTCAM-APX) operated at a speed of 8,000 frames per second with effective pixel size of 640x128 with a Nikon 60mm f/2.8D Micro-Nikkor lens was used to capture the images of the spray. The captured images were processed in order to calculate a number of spray characteristics such as the spray tip penetration, spray cone angle together with spray radial and height (thickness) travelling along the wall foot-print. The spray edges were detected by

using a digital imaging program using a specified threshold level to distinguish the spray edges from background. A typical unprocessed image is shown in Fig. 3.12. The threshold was applied to the images to detect the outline from the background. The chosen threshold level was selected from one image from a batch of images by varying the threshold to obtain optimum results. This threshold value was used for all the images in the same batch.

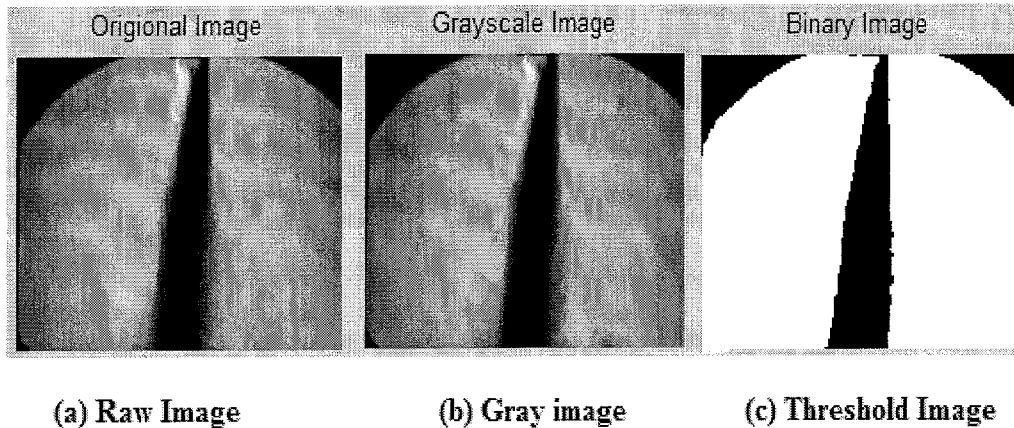


Figure 3.12: unprocessed digital spray image (a & b) and image after applying the threshold (c).

In order to compare the characteristics of the diesel single fuel to the diesel-CNG dual-fuel, the threshold value was kept constant for both batches of images since the condition of the experiments remained the same during a test run. In the literature there are many definitions for spray tip penetration, in the present work, the spray tip penetration was measured along the centerline axis of the spray as the distance between the injector nozzle tip and the furthest spray point, which was determined by a chosen threshold level and spray axis.

No consensus was found in the literature on the definition of a spray (cone), equivalent spray angle or standard angle. The spray angles were measured by drawing a horizontal line at 20mm from the nozzle tip and the angle between the edges of the spray was measured [30]. Fig.3.13 shows how the spray tip penetration and spray cone angle were defined. Spray impingement was defined as the travel of

the spray along the wall in terms of radial penetration and spray height [50] as shown in Fig. 3.14.

The spray tip velocity was estimated from two consecutive spray images using the tip penetration difference divided by the time difference between the two images [51] as shown in the following equation:

$$U_s = \frac{S_2 - S_1}{t_2 - t_1} \quad (3.5)$$

Where U_s is spray tip velocity (m/s), S is the spray tip penetration (mm) and t is time (s).

To convert pixel measurements to SI unit a calibration image of a graduated scale was taken. In this study, the value of one pixel was found to be equivalent to 0.27 mm.

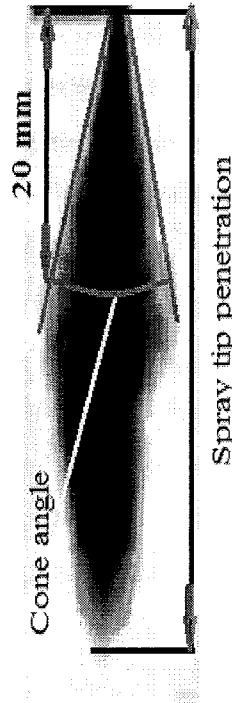
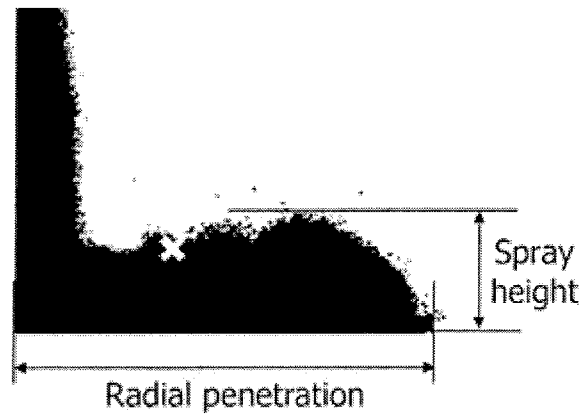


Figure 3.13: Definitions of spray tip penetration and cone angle.



(b) Processed image

Figure 3.14: Definitions of spray radial penetration and spray height [50]

CHAPTER 4

RESULTS AND DISCUSSIONS

This chapter presents the results of an experimental investigation on the propagation of fuel jets created by combined injectors i.e. the CNG injector (low-injection pressure) and a common rail diesel injector (high-injection pressure) using the Schlieren technique for flow visualization of the jets.

In the experiment, the parameters such as the different injection pressures, ~~injectors to wall distance and wall temperatures for the CNG jet, diesel spray and~~ diesel-CNG dual fuel jet were varied to study their effect on the rate of penetration, cone angle, tip velocity and the jet-wall impingement.

In order to present the effect of the CNG jet on the diesel spray, a CNG jet was visualized and the development of its macroscopic jet characteristics were measured together with temporal presentation of the jet wall interaction. In the second section, a diesel spray was visualized and compared to the diesel-CNG dual fuel jet under the same conditions. All acquired images were processed using to obtain the spray tip penetration, spray cone angle and spray velocity together with temporal presentation of the radial travel of the impinged jets along the wall.

4.1 Development of the Comperessed Natural Gas Jet

Figure 4.1 shows the development of the CNG jet created using CNG injector at 18 bar injection pressure and 80 mm injector to wall distance. The images were obtained using a high speed video camera trigged at the start of injection. The start of injection (SOI) is defined as the moment of the solenoid valve closure in the electronic diesel injector as in a common rail diesel injection system. It is different

from the starting of the jet (SOJ), which is defined here as the first visible appearance of the jet emerging from the nozzle.

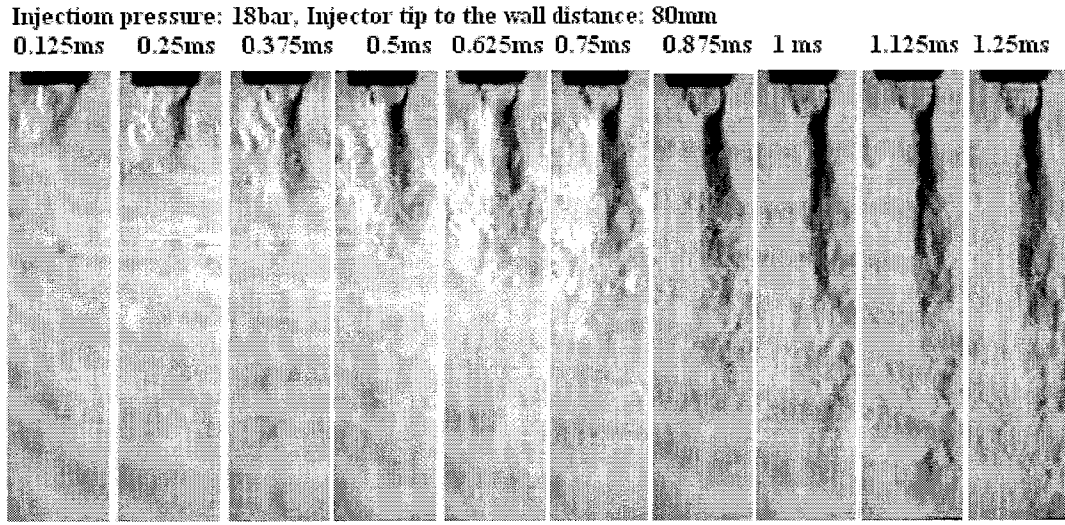


Figure 4.1: Schlieren images of spray pattern of CNG at 18 bar injection pressure and 80 mm injector to the wall distance.

At the initial stages the CNG jet (from 0.125~0.625ms) the development of the gas jet structure a wider jet cone angle which was thought to be due to low momentum of the gas jet as the injectors opened. This matter will be discussed in the following section. This lower gas jet momentum also lead to a lower initial rate of jet tip penetration. As time elapsed, the rate of jet tip penetration increased. It was also noticed that the concentration distribution of the gas at the upstream region became lower in the last images as compared to the first images. The main mechanism for a free jet movement was explained by [52] who divided the jet into two main regions, namely the development region which is continued with a constant mean velocity up to the end of the jet potential core; and the fully developed region which began from the end of the core region. The edge of the jet was not straight because of a turbulent mixing process and entrainment of the flow from the still ambient air.

However, a high fluctuation region was observed at the initial stages of the jet tip as it could be easily influenced by the surrounding air. This phenomenon is quite different than the diesel fuel spray which is not easily influenced by the surrounding air at the initial stages. The reason is that the flow rate of the diesel fuels is high,

and their higher viscosity leads to liquid core having high momentum at start of the injection. This matter will be presented in the following section.

4.1.1 Effect of injection pressure on the CNG jet penetration

Figure 4.2 shows the Schlieren images of the CNG jet under both ambient conditions and different injection pressures (18, 16, and 14 bar), the time intervals from 0.25ms to 1.25ms at increments of 0.25ms. As shown in the jet images, the injection pressure had a large influence on the jet structure as expected [38, 40, 53]. However, with increased of the injection pressures, the delivery time was reduced. It can be said that the high injection pressure had a strong influence on the fuel delivery time as shown in the Fig 4.2 (at 0.75ms). At the initial jet stages, the ~~discrepancy of the penetration was quite small between their different injection~~ pressures (18, 16, and 14 bar), but this differences became more significant as time elapsed. This phenomenon was thought to be caused by the high flow rate leading to a high momentum of the CNG jet. In other words, the CNG jet became strong enough to overcome the resistance of ambient air. Furthermore, it was also noticed that the difference in the jet tip penetration between 18 bar and 16 bar were small in comparison with the differences between 16 bar and 14 bar as shown in Fig. 4.3. Based on this trend, it can be reasoned that, at 18 bar and 16 bar the jet momentum became strong to overcome the resistance of air medium than that of 14 bar. It was also noticed that the lower injection pressure (14 bar) not only lead to short tip penetration, but also resulted in higher concentration region in the center of the jet. The main reason was thought to be again the lower injection pressure leads to lower air-entrainment between the CNG fuel and the air. This is resulted in less mixing. The main mechanism for air-entrainment into the flow can be seen in reference [52].

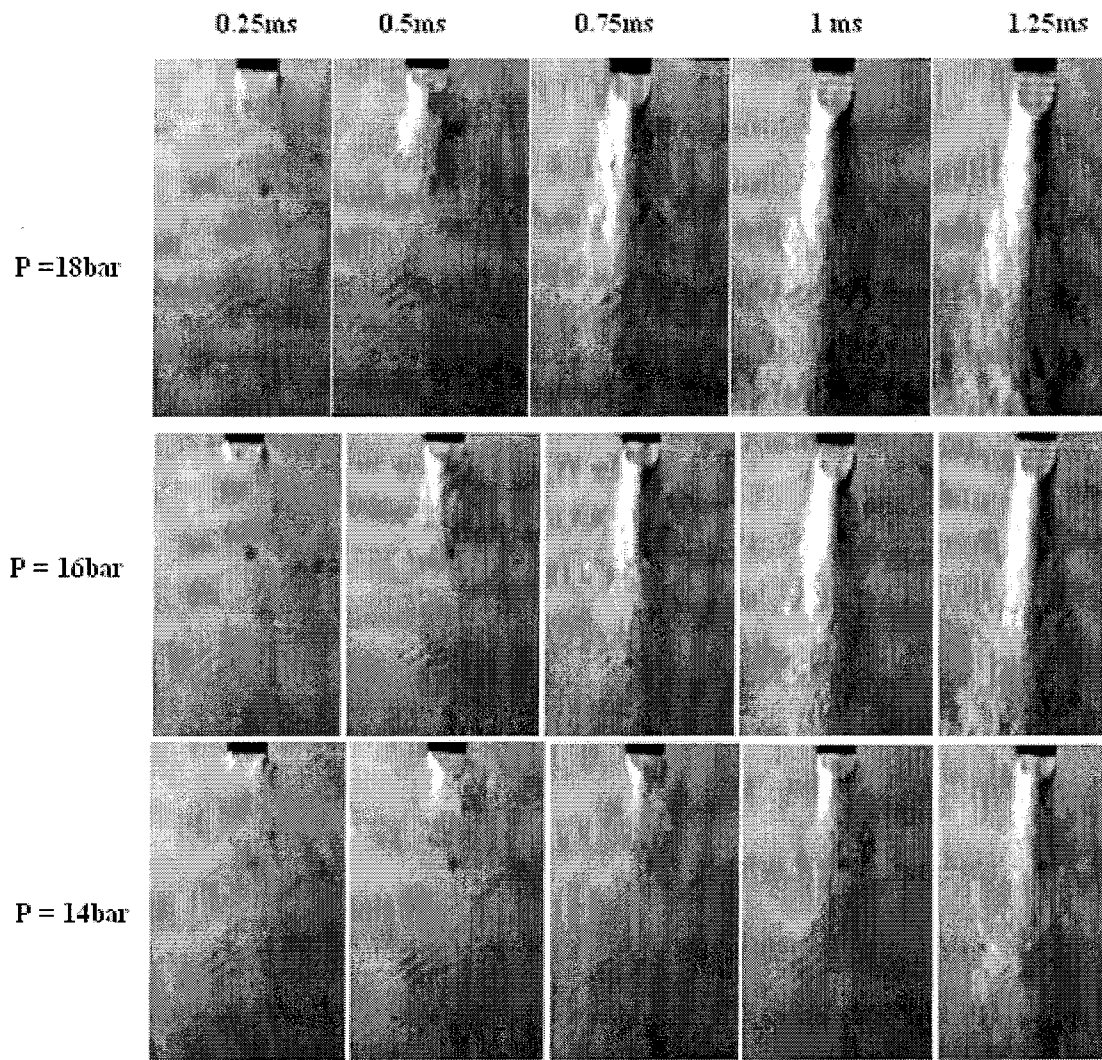


Figure 4.2: Schlieren images for CNG jets at different injection pressures (18, 16 and 14 bar) and 80mm injector to the wall distance.

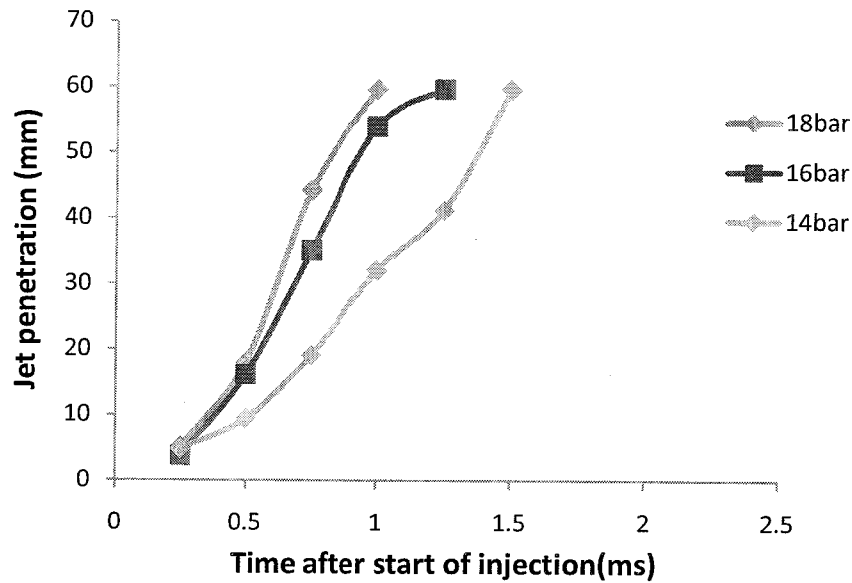


Figure 4.3: The effect of injection pressure on the CNG jet tip penetration at injection pressures: 18, 16 and 14 bar, and injector wall distance: 80 mm.

4.1.2 Effects of injection pressure on the CNG jet Cone Angle

Fig. 4.4 shows the measured spray cone angle against time after the start of injection. The jet cone angle was measured at a distance of 20 mm from injector nozzle. The jet cone angle generally started with a wider cone angle, before reaching a constant value as the jet develops in which was in agreement with most results presented in the literature. It can be seen that at the initial stages (Fig. 4.2) the CNG jet showed an intensely turbulent flow as evident at the sides and the jet tip. This was thought to be the reason for a wider cone angle at start of injection. The reason again were that the jet could be easily influenced by the surrounding air and the high momentum exchange. As time elapsed, the flow rate increased and resulted in a less turbulent flow, hence, the cone angle decreased and reached a constant value. This type of behavior was also seen in the diesel fuel spray which have lower cone angles compared to gaseous jets.

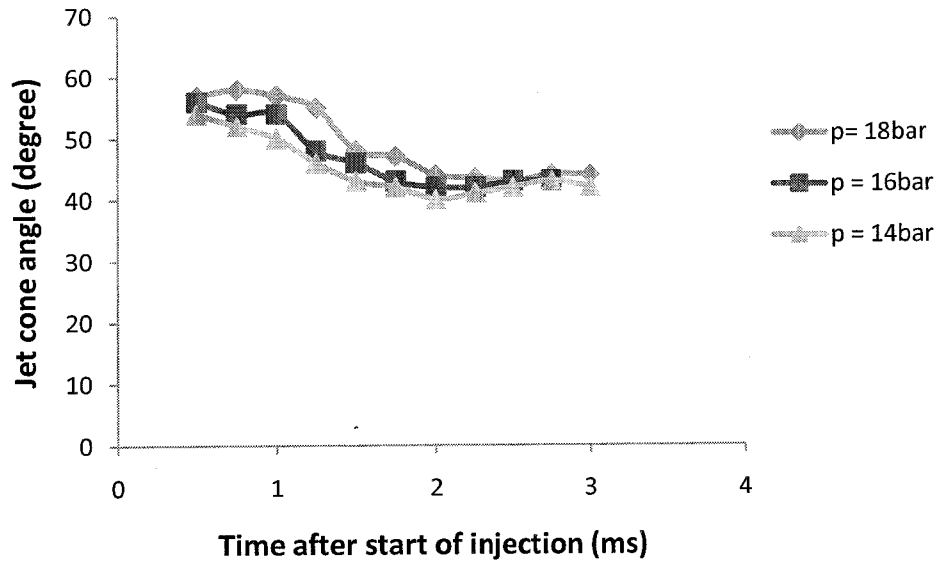


Figure 4.4: the effect of injection pressure on the CNG jet cone angle at injection pressures: 18, 16 and 14bar.

4.1.3 Effect of injector-wall distance on the jet tip penetration

Figure 4.5 shows the effect of the wall distance from the injector on the jet tip penetration. It can be seen that the tip penetration rate decreased in the axial direction as the jet travelled with the increase of the injector to the wall distance. This phenomenon is thought to be by the effect of the aerodynamic resistance which increased with an increase of the jet cone angle and a loss of the jet momentum due to air entrainment by the jet.

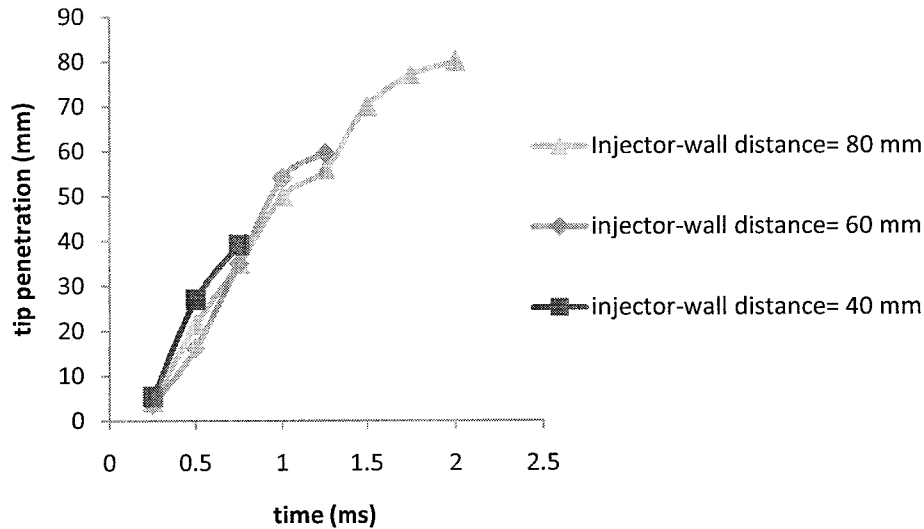


Figure 4.5: The effect of the injector-wall distance on the jet tip penetration against time.

4.1.4 Effects of Wall impingement on the CNG jet development

The jet wall impingement is the most important characteristic influencing the jet mixing process. Fig. 4.6 shows the CNG jet impingement at 40 mm injector tip to wall distance and 18 bar injection pressure. It can be seen that the free jet tip arrived at the impingement wall 1 ms after the start of injection. Also it can be seen that, at the initial stages of the development of the gas jet on the wall, both the jet tip velocity and momentum considerably decreased. Thus, the CNG was observed to accumulate on the wall. As time elapsed, the accumulated CNG was pushed by the following CNG flow resulting in a radial and axial spread along the wall from the impingement point. The spreads of the impinged jet on the wall was found to form a vortex core as a result of air resistance in front of the spreading jet tip which formed into a large scale jet structure increasing with the elapsed time as a result of the air-entrainment in the wall.

The CNG jet-wall impingement can be explained based on the development of the radial spread on the wall and the jet height. The radial penetration here was defined as the radial distance from the jet axis at the impingement wall to the end of the gas jet tip,

while the jet height (thickness) was defined as the furthest jet points (in the axial direction) after the jet impingement as shown in Fig. 4.7.

At the initial stages, the CNG jet was highly turbulent at the sides of the jet resulting in a lower penetration rate along the wall. The phenomenon was thought to be caused by the instabilities of the shear layer because the mixing of the CNG and the entrained air was rolling up the CNG vortices. However, the shear layer thickness (height) grew with downstream distance. In this region the concentration field was broken resulting into lower jet height and secondary vortices with high concentration in the region [54].

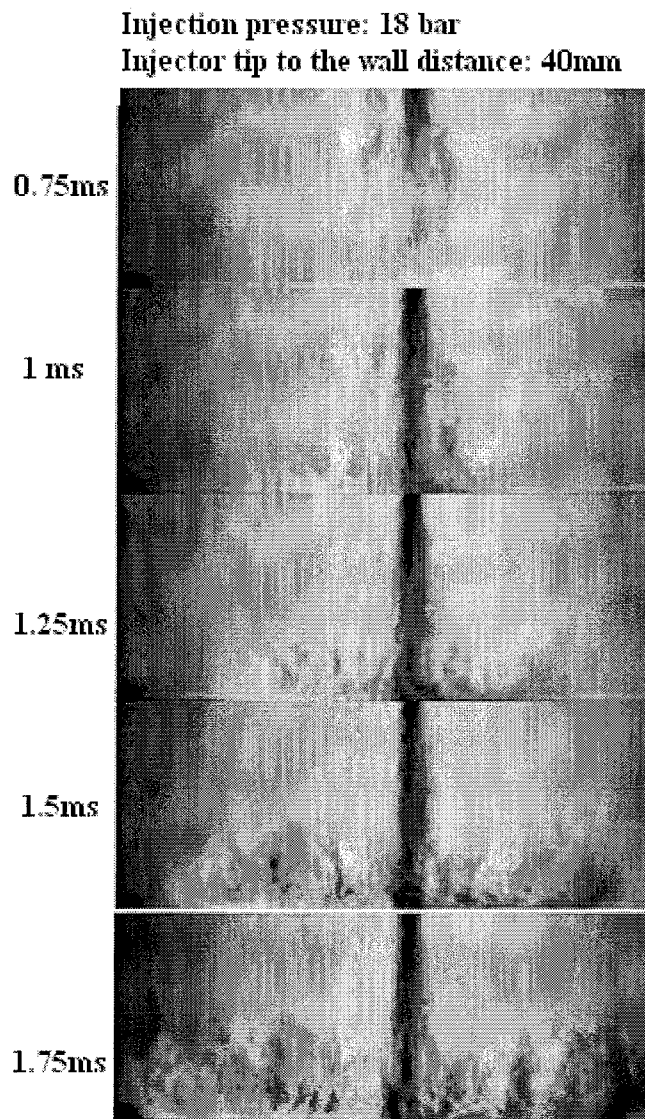


Figure 4.6: CNG jet-wall impingement at injection pressure: 18bar and injector to the wall distance: 40mm.

Generally, the formation of vortex structure in the CNG jet can be analyzed as the jet tip (vortex core) radial penetration along the wall and their heights (thickness) as explained by Ding et al. [55] who defined the concentration core based on the normalized concentration versus radial direction from the impingement point.

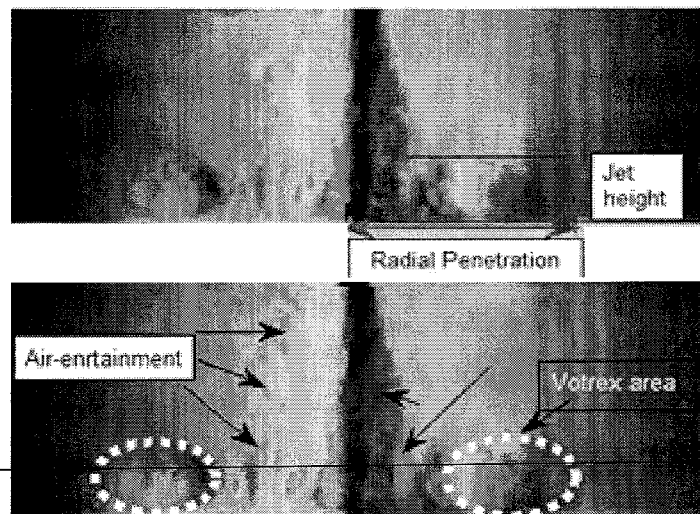


Figure 4.7: Concentration field of CNG jet

Fig. 4.8 shows the development of the CNG jet on the radial penetration and the jet height at injection pressure 18 bar and injector to the wall distance 40 mm. It can be seen that the impinged jets were initially focused on the radial wall penetration rather than the jet height (before the deflection of the mixing layer which resulted in a secondary vortex). This could be explained as follows: The mixing layer spread to the both potential core and the ambient fluid flow, hence, leading to more uniform concentration profiles. With elapsed time, the tip vortex roll up increased with the large scale motion resulting in a higher radial wall penetration and the jet height. These resulted in a dominant mechanism for air entrainment and a large-scale engulfment of the surrounding air by the vortical structures, and both the jet and the entrained air mixed rapidly [52].

This phenomenon is completely different in the diesel fuel sprays for non-evaporating conditions i.e. high momentum, large droplets and evaporation; hence, the air resistance becomes lower resulting in the similar heights of the impinged spray [50].

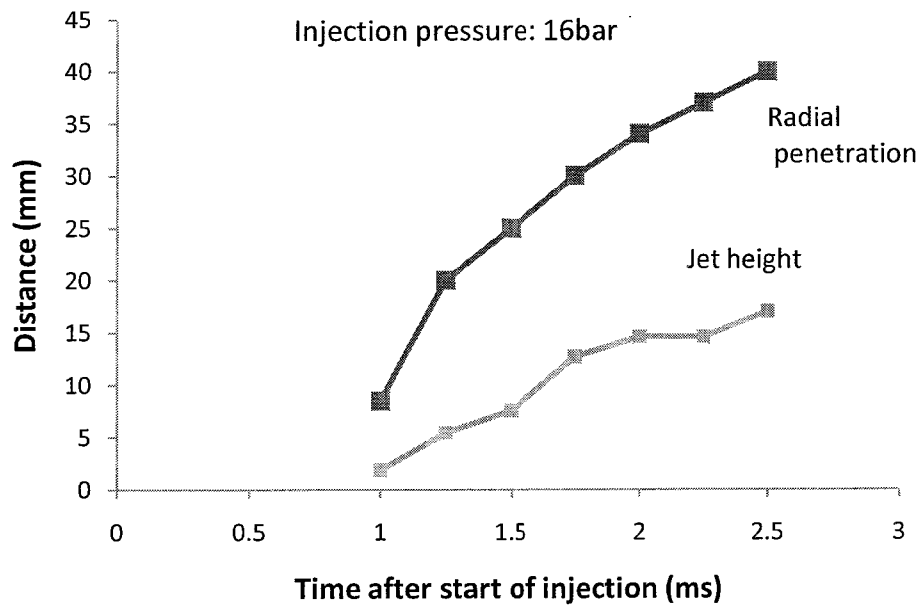


Figure 4.8: Development of the CNG jet impingement (radial penetration and jet height) along the wall versus time

4.1.5 Effect of injection pressure of CNG jet on the Wall-impingement

To investigate the effect of injection pressure on the concentration and the distribution along the wall, three injection pressures (18, 16 and 14 bar) were used in this study. Fig. 4.9 shows the effect of injection pressure of the CNG jet along the impingement wall (radial penetration). As expected, it can be seen that the injection pressure increased, the radial penetration of the jet tip along the wall was increased. The phenomenon was thought to be caused by the effect of the higher momentum of at the moment of impingement. It is generally accepted that the jet radial penetration motion is vitally important for the jet mixing process as it enhances the lower penetration of the jet by creating turbulent energy. The friction resistance of the wall and the pressure resistance from the surrounding are considered as the main reasons. This is necessary for molecular mixing with small-scale motion in the subsequent mixing process [56]. On the other hand, the CNG jet height development on the wall is shown in Fig. 4.10. It can be seen that the jet height can be increased very quickly at the moment of impingement, and the higher injection pressure has a higher impingement height. Also it can be seen that after the jet height grew before reaching

an almost constant value. At this stage initial vortex was vortex broken and followed by secondary vortices.

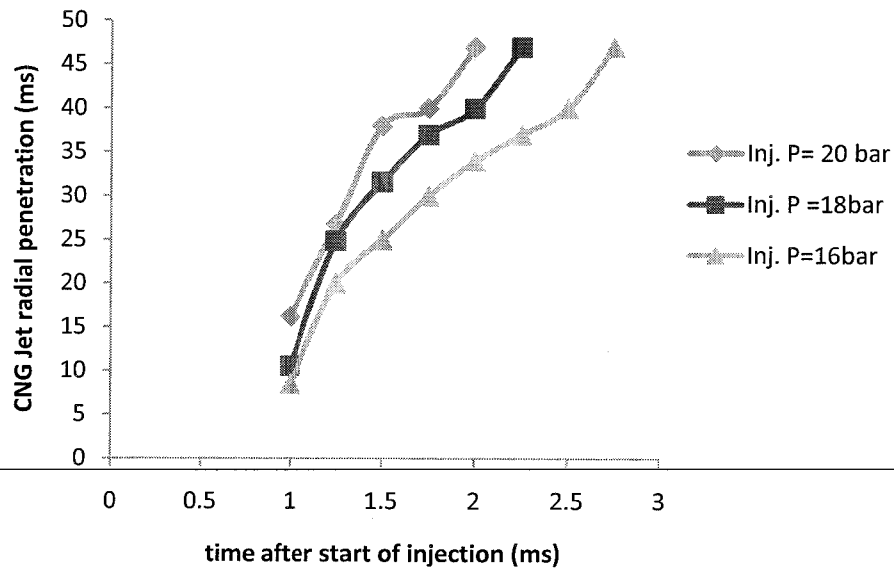


Figure 4.9: Effects of different injection pressures (18, 16 and 14bar) along the Wall-impingement at 40mm injector to the wall distance.

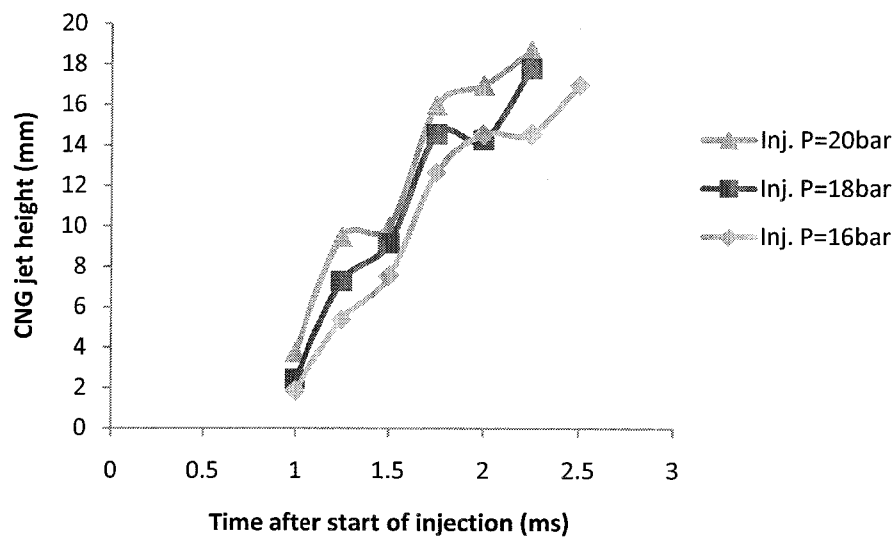


Figure 4.10: Effects of different injection pressures (18, 16 and 14bar) on the height along the Wall-impingement at 40mm injector to the wall distance.

4.2 Spray Characteristics of Diesel and Diesel-CNG Dual Fuel Jet

4.2.1 Spray Tip Penetration Measurements

Fig.4.11 represents the spray evaluation process of the diesel and the diesel-CNG dual-fuel ranging from 0.125ms to 0.75ms after the start of injection. In order to compare the images of the diesel spray (single fuel) and diesel-CNG dual fuel jets, the process of the same threshold levels were used to distinguish the spray edges from the background, since the quality of images remained the same during the test runs. The spray tip penetration rate for both fuels increased with elapsed time. It can be seen that, most of the upstream region of the spray did not reach its fully developed shape which was in agreement with previous study [10]. The rate of penetration of the diesel spray in the dual-fuel case was relatively longer in the upstream part than that of the diesel single fuel. This probably due to the low CNG jet momentum, having a minimal effect on the high momentum diesel spray (see section 4.1). This phenomena was also observed by [57] who suggested that the exchange of energy was higher at the beginning of the injection when the air began to be entrained. As time elapsed, the rate of penetration of the dual-fuel was higher than that of the diesel single fuel as a result of energy transfer between the sprays. These results agree with recent findings [57-58] in which their conclusions were that, the droplets located in the spray tip were influenced by both shear force (shear between the surrounding gas) and the spray envelope. Following these influences, the particle trajectories were entrained towards the spray periphery. In other words, the small size droplets approached the same velocity which was the velocity of the carrier phase rather than the uncorrelated motion produced by shear or compression.

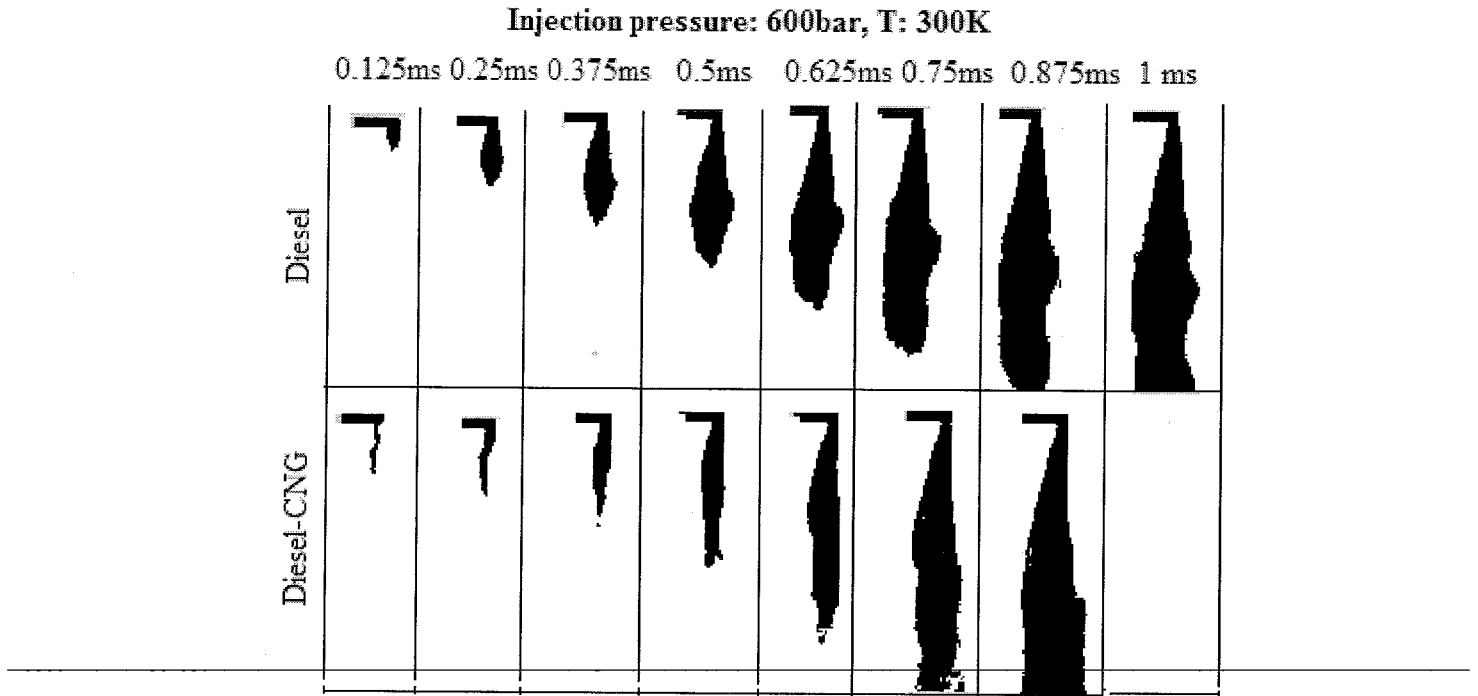


Figure 4.11: Schlieren images for diesel and diesel-CNG dual fuel at injection pressure: 600, 18 bar for diesel and CNG respectively and the injector wall distance: 80 mm.

4.2.2 Spray tip velocity measurements

The jet velocities of the diesel and diesel-CNG dual-fuel are shown in Fig. 4.12. It can be seen that, in the first phase, both spray tip velocities were slower as expected, due to the effect of the drag force produced by the ambient gas. As time elapsed, the diesel-CNG dual jet showed a higher tip velocity (138 m/s), compared to the pure diesel spray (120 m/s). The reason for this phenomenon can be explained by a reduction in the aerodynamic interaction with the ambient gas. In other words, the diesel spray droplets momentum was enhanced by the CNG axial velocity as their kinetic energy increased, where the CNG jet has caused the breakage of larger size spray droplets of diesel fuel and this caused a higher velocity as well as higher momentum and lower resistance due to the fact that the higher momentum is transferred into higher kinetic energy. The phenomena of diesel velocity profile was studied by [60] who noticed that, both the droplets velocities and diameters were largely influenced by the flow momentum, where the droplets diameter were small

with the high momentum. At the downstream region, both the spray tip velocities again lost their momentum and became slower, while the diesel spray in the dual fuel was higher. The reason was probably the same as described before. The study also found that the injection velocity was higher than the spray tip velocity.

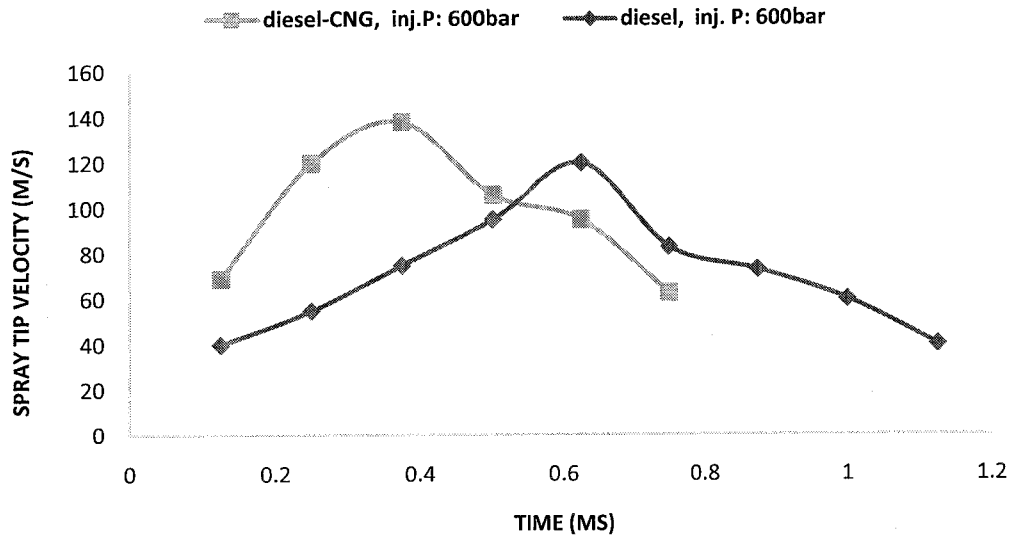


Figure 4.12: Spray tip velocity of diesel and diesel-CNG dual fuel jet at injection pressure: 600 and 18 bar for diesel and CNG respectively and the injector to the wall distance: 80 mm.

In order to better understand the difference between the spray tip velocity of diesel single fuel and diesel-CNG dual-fuel, the diesel injection pressure was changed to different injection pressures (500, 600 and 700 bar) while the CNG pressure remained constant as shown in Fig. 4.13. It can be seen that, as expected, the spray tip velocities increased as the injection pressure increased, in agreement with most of the results presented in the literature [10, 60] where the higher injection pressure was transferred to higher kinetic energy. Also it can be seen that the divergence of the curves are all similar, but the differences between the injection pressures 700 and 600 bar for diesel-CNG dual-fuel was less than that of the 600 and 500 bar cases. Based on this trend, it can be reasoned that the CNG jet became less effective with increasing the diesel injection pressure.

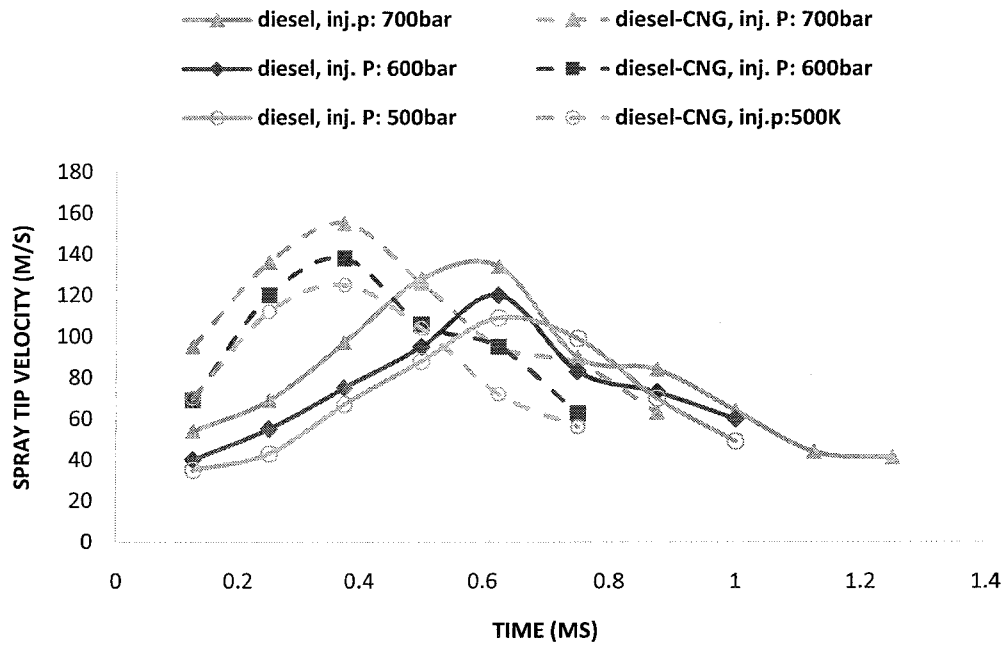


Figure 4.13: Spray tip velocity of the diesel and the diesel-CNG dual-fuel jet at different injection pressures (700, 600 and 500 bar) for diesel spray and 18 bar for the CNG jet and injector wall distance: 80 mm.

4.2.3 Spray cone angle measurements

The development of the spray cone angle with time for both the diesel and the diesel-CNG dual-fuel are shown in Fig.4.14. In agreement with results in the literature, the diesel spray cone angle decreased at the initial stages before reaching a constant fully developed value. Actual values of the spray cone angle were in the range between 8° to 40° depending on the fuel specification, nozzle geometry and the ambient gas density and temperature [31], this was similar to the values found in this study. The results also showed that the spray cone angle of the pure diesel was greater than that for diesel-CNG jet at the initial stages, later, this difference became very small. This was thought to be due to the effect of the CNG jet on the diesel spray, where the diesel flow rate was lower at the initial stages resulting in the CNG jet becoming more effective in the axial direction. Also the reason was probably again produced by the compression of the CNG jet on the diesel spray which resulted in a lower spray cone angle with higher spray tip velocity and penetration as shown in Fig. 4.10 and 4.11.

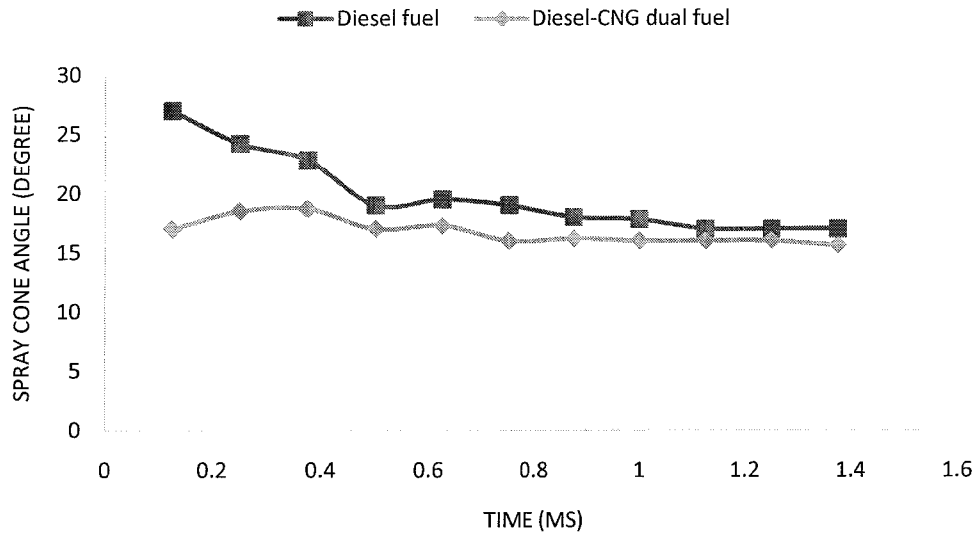


Figure 4.14: Spray cone angle of diesel and diesel-CNG at injection pressure: 600, 18 bar for diesel and CNG respectively and injector wall distance: 80 mm.

4.2.4 Temperature effects

Before the experiment started, the temperature distribution inside the rig was measured and showed that there was a moderate gradient from bottom to top. When the bottom plate was heated up to 500°K, the temperature variations were 72, 64, 60 and 54°K at 20, 40, 60 and 80 mm from the bottom plate respectively. The ambient temperature inside the chamber was calculated from the average values of the temperature variation.

4.2.4.1 Spray Tip Penetration Measurment

The spray tip penetrations under different temperatures (300, 400 and 500°K) are presented in Fig.4.15 for both diesel and diesel-CNG dual fuel. The rate of spray tip penetration was reduced in both cases as the ambient temperature increased which was in agreement with the findings of Taşkıran and Ergenman [10]. This was caused by the loss of momentum of the jet due to the liquid evaporation. The temperature effect on the diesel spray tip penetration was relatively more significant than that on the diesel-CNG dual-fuel jets as a result of the higher evaporation rate of the diesel jet in

the

absence of the CNG. Furthermore, it can be seen that, in the case of diesel spray (single fuel), the profiles for both charge-temperature (400°K and 500°K) diverged after 0.5ms from the start of injection. The rate of diversion increased as the temperature increased. While in the case of dual fuel, the effect of charge temperature on the spray rate of penetration was not as significant. This may be due to the temperature gradient in the direction of the jet penetration having a greater effect in the absence of CNG. This was due to the fact that the effect of temperature became lower as the mass quantity (diesel+ CNG) increased. The findings of this work on penetration rate (liquid phase under evaporation) with time agree with both Kennaird et al. [26] and Sazhin et al. [61] who found that the penetration was linear with time. The main reasons for the vapour jet transport was the losses of the momentum of the jet by the surrounding air motion as suggested by [10, 62].

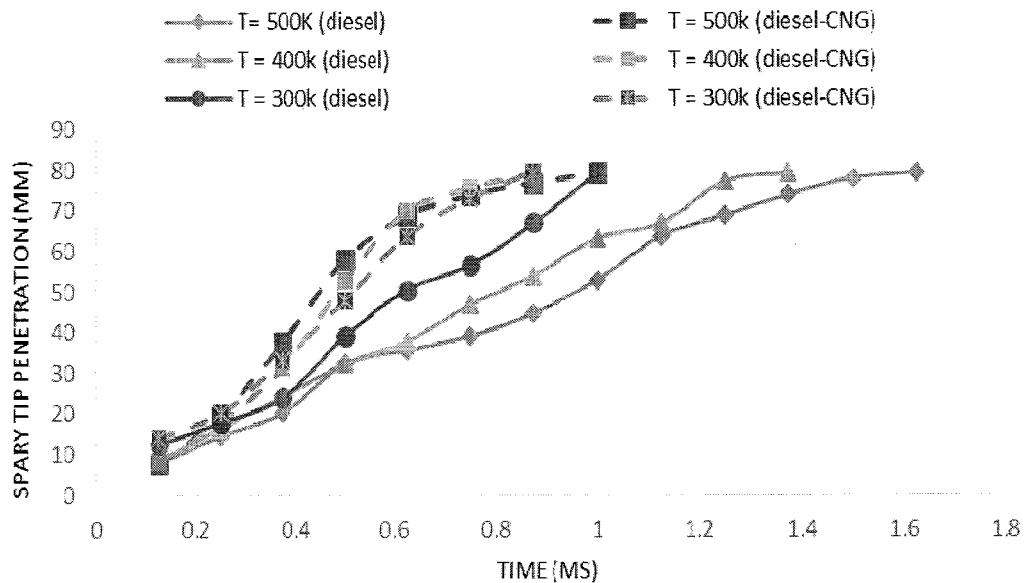


Figure 4.15: Effect of different temperatures (500, 400 and 300 °K) on the diesel and diesel-CNG dual fuel at injection pressure: 600 and 18 bar for diesel and CNG respectively.

To go further in the comparison between sprays of single diesel fuel and diesel-CNG dual fuel, the diesel injection pressure was changed to 500, 600 and 700 bar at 500°K temperature as depicted in Fig.4.16. As expected, the results showed that the highest rate of penetration was found to occur with the highest injection pressures.

The results also showed that the diesel spray (single fuel) started to diverge earlier than that of the diesel-CNG dual-fuel. This was probably caused by the effect of the CNG jet velocity in the axial direction which was higher than the effect of the temperature profiles. Also it can be noticed that the differences in the tip penetration between injection pressure 500, 600 and 700 bar in diesel spray (single fuel) were greater in comparison with the differences between same pressures in the diesel-CNG dual fuel case. Based on this trend, the main reason was probably again related to both quantity and the axial velocity of the diesel spray influenced by the relative velocity of the CNG jet more than that of ambient air as in single diesel spray, Hence, the droplet penetrated faster. This mechanism was studied by Martinez and Benkenida [57] who observed that the droplets velocities gradually approached that of the carrier phase. They suggested that, in evaporating sprays, the characteristics time of evaporation is so small compared to the follow through time. Furthermore, the effects of profile temperature on the droplets in both cases are greater at low injection pressure. This is can be reasoned by the diesel spray being less dense at high injection pressures [28], in addition, the higher injection pressures generate small droplets and increase the rate of fuel delivery time. Hence, resulted in a reduction in the rate of evaporation and heat transfer.

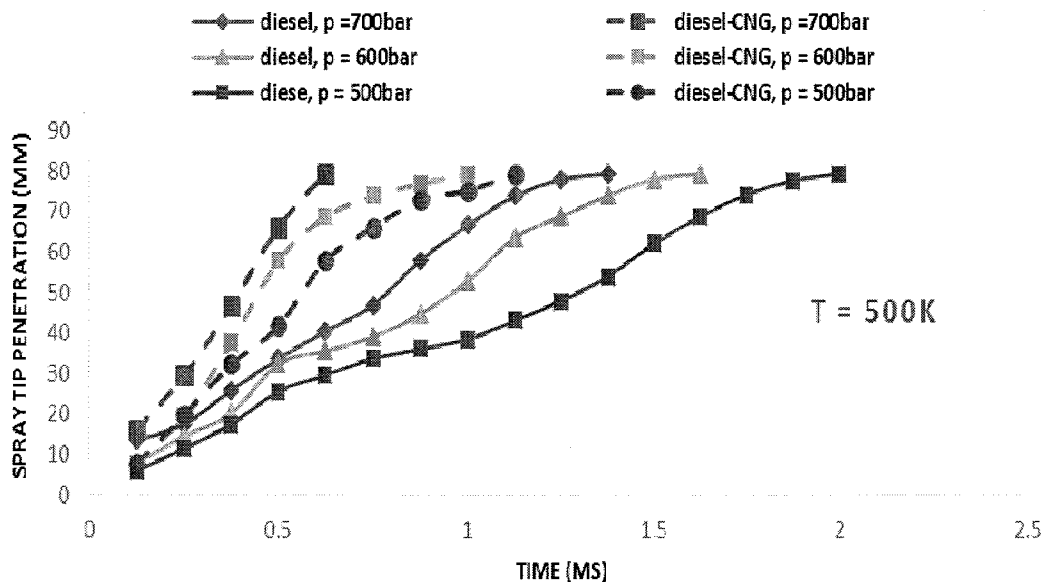


Figure 4.16: Effect of different injection pressures (500, 600 and 700 bar) on the diesel and diesel-CNG dual fuel at 500 K wall temperatures.

4.2.4.2 Spray cone angle measurement

Fig. 4.17 shows the effect of different wall temperatures (300, 400 and 500°K) on the spray cone angle of the diesel (single fuel) and the diesel-CNG dual fuel. The diesel and the CNG injection pressures were 600 bar and 18 respectively with time after start of injection. The effect of temperatures on the spray cone angles for both diesel and diesel-CNG dual fuel were found to increase with the increase of temperature. It can be seen that, the diesel-CNG dual fuel had a lower spray cone angle with a lower temperature in comparison to the absence of CNG, and this difference become small with increasing the temperature (at temperature: 500°K, their spray cone angle became approximately equal). The reason of the lower cone angle of the dual fuel at low temperature was probably due to the effect of the CNG jet in the axial direction resulting in a high spray tip penetration rather than spray cone angle. On the other hand, at the higher wall temperature, the dual fuel spray cone angle become wider probably due to the momentum exchange between the fuel droplets and the CNG jet becoming high at higher temperature.

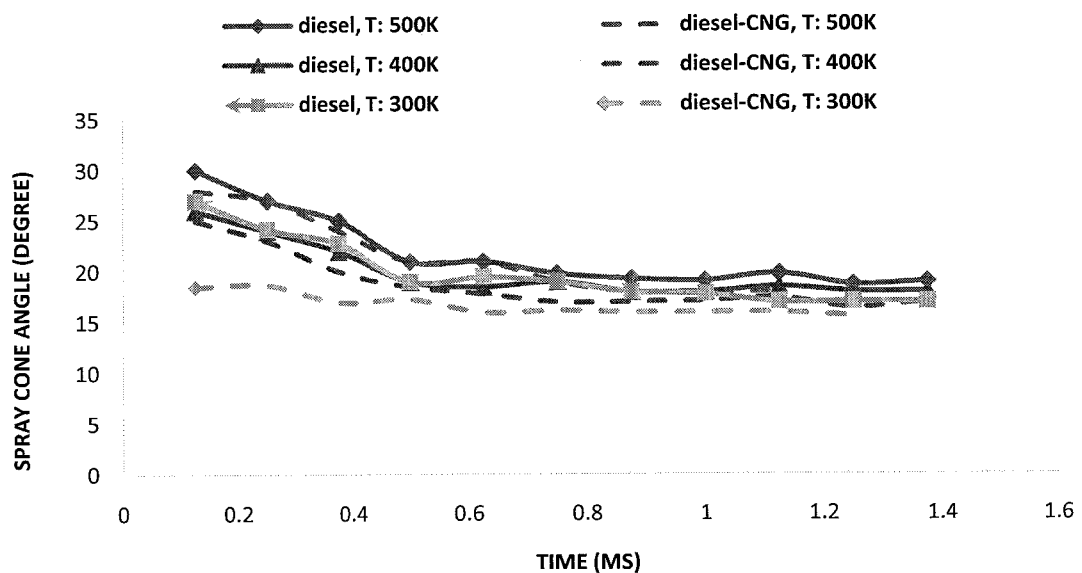


Figure 4.17: Spray cone angle of diesel and diesel-CNG dual-fuel at different wall temperatures (500, 400 and 300°K) and the injection pressure: 600bar and 18 bar diesel and the CNG respectively.

4.2.4.3 Spray tip velocity measurement

Fig. 4.18 shows the spray tip velocity for diesel and diesel-CNG dual fuel at different wall temperatures (500 and 300°K), injection pressure 600 and 18 bar for diesel and CNG respectively and injector to the wall distance 80 mm. It can be seen that, for an increase in the temperature, an increase in the spray tip velocity was observed for both causes. As expected, the velocities increased due to the high temperature leading to a decrease in the droplet diameter which reduces the aerodynamic drag [12]. The results also showed that the jet tip velocity of the diesel-CNG dual fuel was higher than that of pure diesel. This trend can be easily observed by looking at diesel-CNG tip velocity at 300°K at 0.625ms after the start of injection, it was 145 m/s compared with 125 m/s under the same temperature as shown in Fig. 4.18. This may be attributed to the fact that the relative velocity between the diesel spray and the CNG jet was higher compared to the relative velocity between the diesel spray (single fuel) to the surrounding gas. In other words, the diesel spray transfers their momentum to the entrained air and decreases rapidly their relative velocities, and at the same time receives heat from the entrained air. While in the case of diesel-CNG dual fuel, the diesel spray gained momentum from the CNG jet while receiving heat from the entrained air. This is resulted in a higher spray tip velocity of the diesel-CNG dual fuel jet.

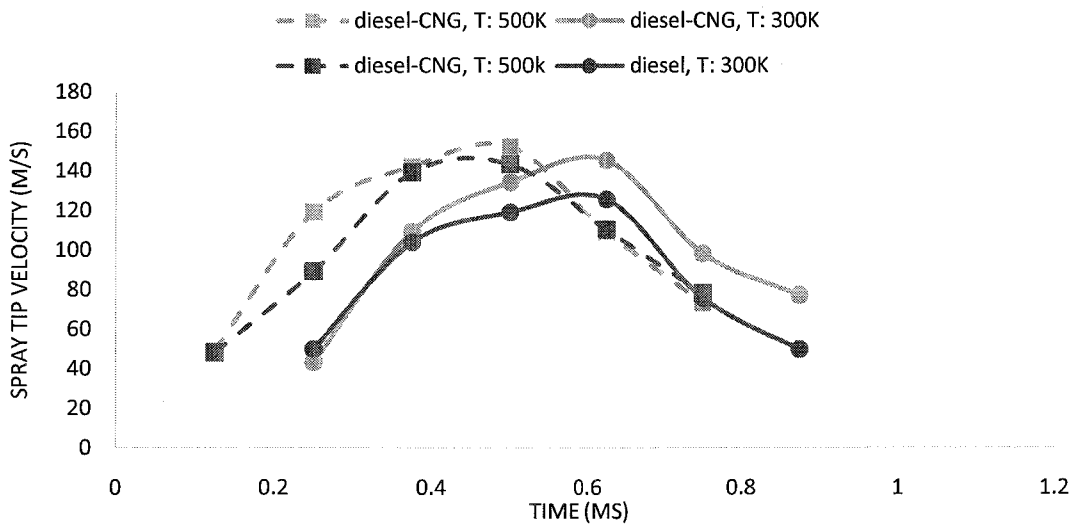


Figure 4.18: Spray tip velocity of diesel and diesel-CNG dual-fuel jet at different wall temperatures (500 and 300K), injection pressure: 600, 18bar for diesel and CNG respectively and injector wall distance: 80 mm.

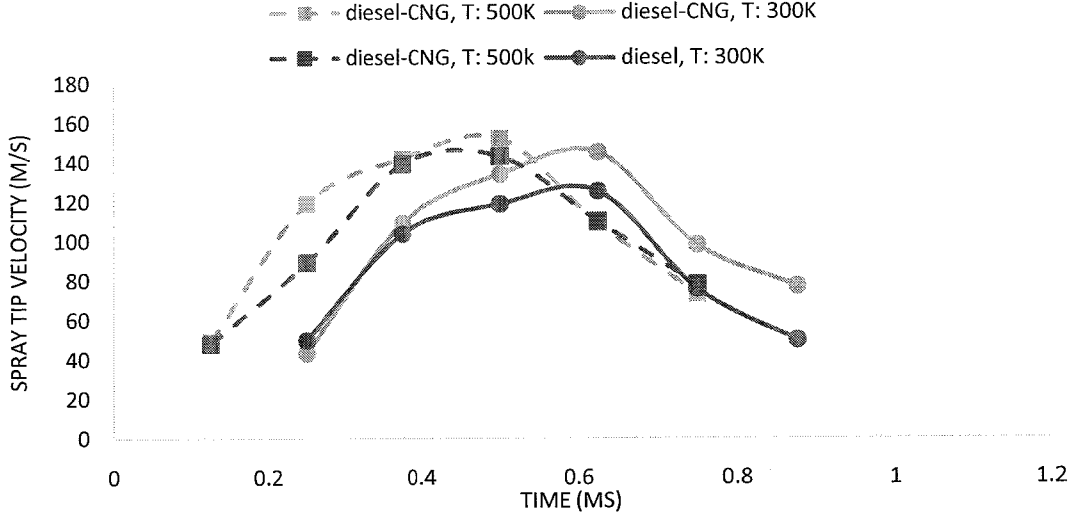


Figure 4.18: Spray tip velocity of diesel and diesel-CNG dual-fuel jet at different wall temperatures (500 and 300K), injection pressure: 600, 18bar for diesel and CNG respectively and injector wall distance: 80 mm.

4.2.5 Calculations of the diesel jet characteristics

Beside the experimental studies, many theoretical and empirical correlations were recommended for the prediction of the diesel spray penetration and the spray velocity. Several correlations have been suggested to determine the spray penetration. When the spray is first injected into the chamber, the initial velocity of the spray tip is much larger than the surrounding air. According to Hiroyasu and Arai [63] at this zone the penetration is described by an expression proportional to time.

$$0 < t < t_b \quad S(t) = 0.39 \sqrt{\frac{2\Delta P}{\rho_f}} t \quad (4.1)$$

$$t > t_b \quad S = 2.95 \left(\frac{\Delta P}{\rho_g} \right)^{0.5} (td_o)^{0.5} \quad (4.2)$$

Where t_b = break up time given by $t_b = \frac{28.65 \rho_f d_o}{(\rho_g \Delta P)^{0.5}}$

S = Spray penetration,

ΔP = pressure drop across the nozzle,

ρ_f = fuel density,

ρ_g = gas density,

t = time,

t_b = break up time and

d_o = nozzle diameter.

Fig. 4.19 shows the comparison between the experimentally observed and the calculated spray tip penetration of the diesel fuel under 600 bar injection pressure.

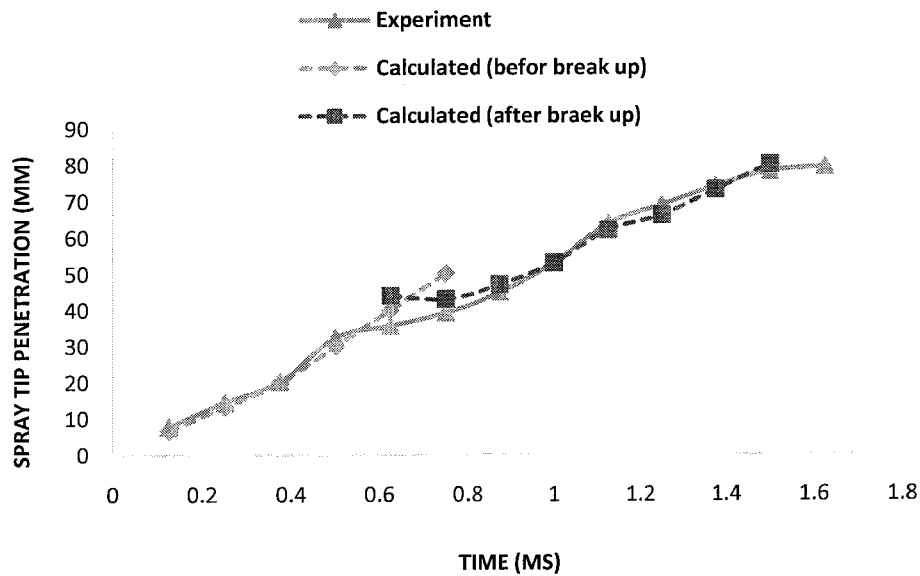


Figure 4.19: Comparison between the experimental and the calculated spray tip penetration of diesel fuel at injection pressure 600bar and ambient temperature.

While Dent [64] developed a formula based on the gas jets theory, where spray penetration depends on the gas density and temperature as following:

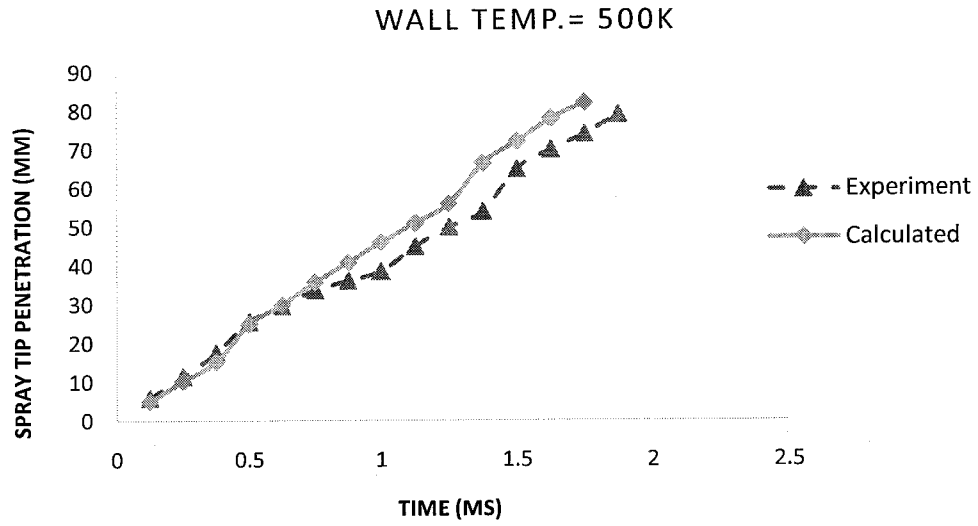


Figure 4.20: Comparison between the experimental and the calculated spray tip penetration of the diesel fuel at injection pressure 600 bar and the wall temperature 500°K.

Spray tip velocities are considered to be dependent upon the injection pressure and the ambient pressure according to Hiroyasu et al. [65] as follows:

$$U_s(t) = \frac{3}{2} \left(\frac{\rho_f}{\rho_a} \right)^{0.25} \left(\frac{\rho_a^{1/3}}{12\rho_f} \right)^{0.5} t^{0.5} \quad 0 < t < t_{break} \quad (4.4)$$

$$U_s(t) = 2.95 \left(\frac{\Delta P}{\rho_a} \right)^{0.25} \left(\frac{(C_f)^z d}{t} \right)^{0.5} \quad t \geq t_{break} \quad (4.5)$$

Where $C_f = \frac{d_i}{d_o}$

And Z is the power of conicity parameter, equals to (-1) for convergent nozzles, (+1) for divergent nozzles and (0) for straight nozzles.

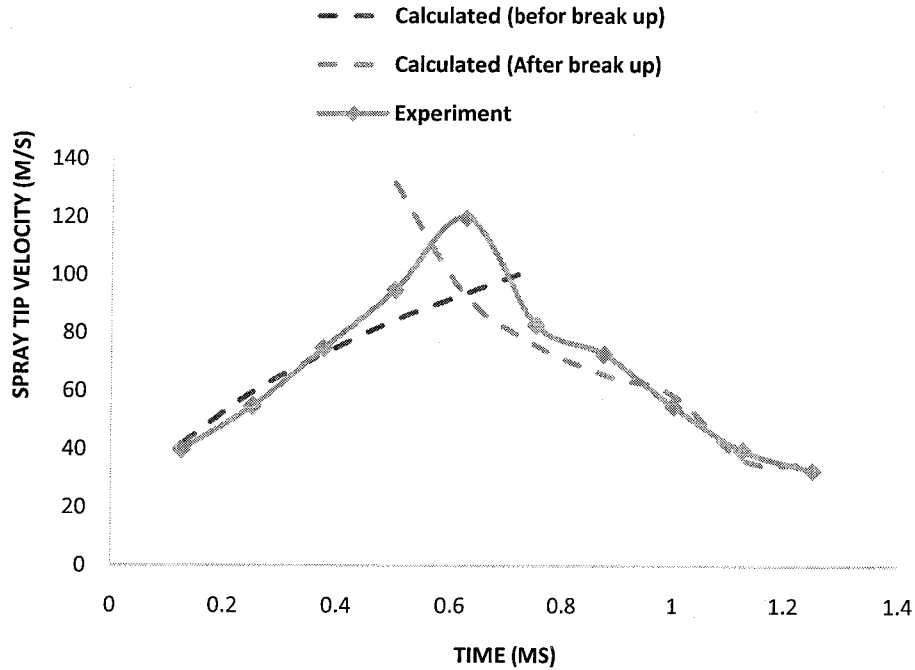


Figure 4.21: Comparison between the experimental and the calculated spray tip velocity of diesel fuel at injection pressure 600 bar at ambient temperature.

It can be seen that the experimental results are in agreement with the Hiroyasu's equation, however, there is also some dissimilarity. This may be caused by the nature of the diesel properties used.

4.2.6 Effects of Wall impingement on the diesel-CNG dual fuel jet development

The jet-wall impingement characteristics seem to be one of the most effective ways to tackle stringent emissions of the diesel engines. In this section, the jet-wall impingement was identified based on the radial penetration and jet height (see section 4.1.3).

Fig. 4.20 shows the comparison between the development of the CNG jet and the diesel spray on the wall. It can be seen that the CNG jet was largely affected by the ambient air due to its low density and momentum.

Fig. 4.20 shows the comparison between the development of the CNG jet and the diesel spray on the wall. It can be seen that the CNG jet was largely affected by the ambient air due to its low density and momentum.

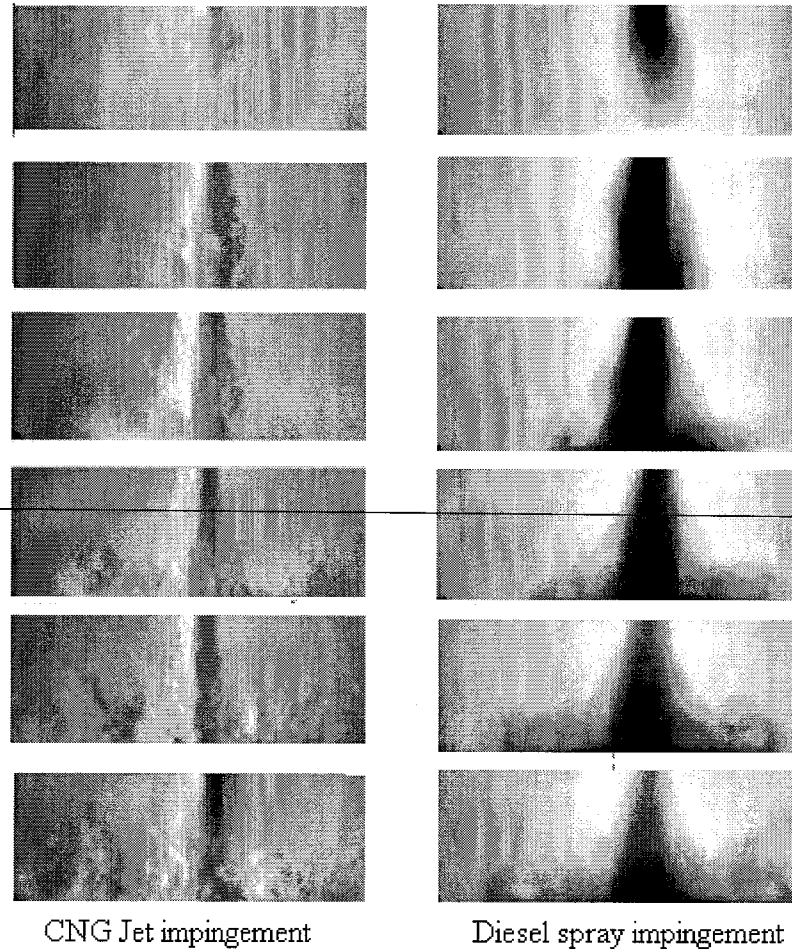


Figure 4.22: The effects of injection pressure on the characteristics of diesel spray and diesel-CNG dual fuel impingement.

The development of the diesel and diesel-CNG dual fuel jet on the radial penetration along the wall and the jet height are presented in Fig. 4.22. The injection pressures of diesel and CNG were 600 bar and 18 bar respectively at ambient wall temperature. It can be seen that the diesel-CNG dual fuel had a higher radial penetration than that of pure diesel. This phenomenon can be reasoned as following: as the pure diesel spray approaches the wall, it losses axial velocity caused by the interaction between the liquid and the wall, while in incase of diesel-CNG dual fuel, the axial velocity was enhanced by the CNG jet resulting in a higher radial penetration on the wall. On the other hand, for the jet height, the pure diesel spray

showed higher height than that of diesel-CNG dual fuel. This was probably due to the CNG jet having a lower density and thus easily mixed with ambient air while the diesel focused on the wall. The findings of this work are consistent with other results sets reported in literature [50].

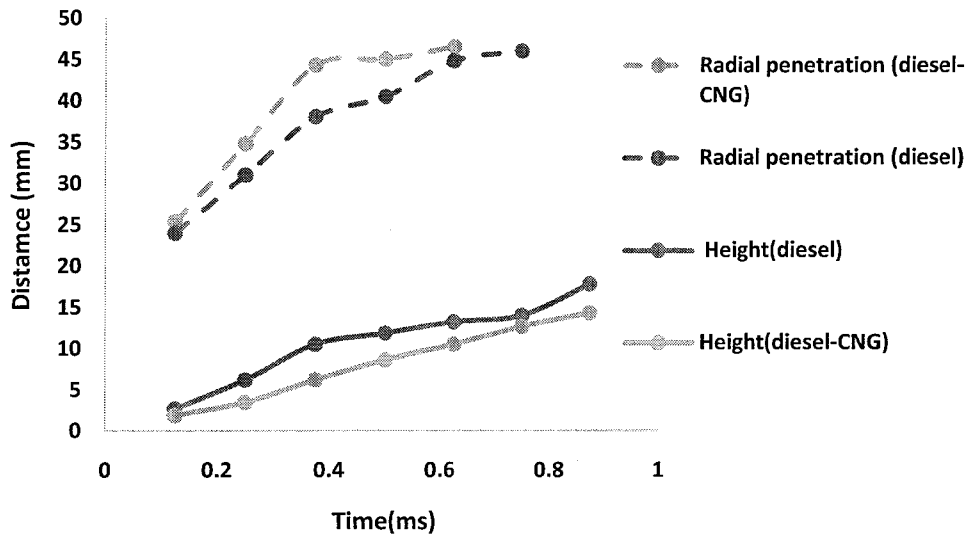


Figure 4.23: The radial penetration and height of diesel and diesel-CNG dual fuel jet impinged on the wall (inj. P= 600 bar for diesel and 18 bar for CNG, 60mm inj. to the wall distance and the wall temperature 400K).

4.2.6.1 Effect of injection pressure on the radial penetration.

The effect of injection pressure on the jet radial penetration along the wall of the diesel and diesel-CNG dual fuel are shown in Fig. 4. 23. In this figure, only the injection pressure for the diesel fuel was varied (500, 600 and 700 bar) because the CNG pressure variation was found to have very small effect in comparison to the diesel pressure. As shown in the figure, both the diesel and diesel-CNG dual fuel showed higher radial penetration with high injection pressure which is a well-known phenomenon. But in comparison between the single and dual fuel, the pure diesel radial penetration was largely affected by increasing the injection pressure rather than that of diesel-CNG. This trend indicates that the diesel fuel loses its momentum by vortices of CNG [55].

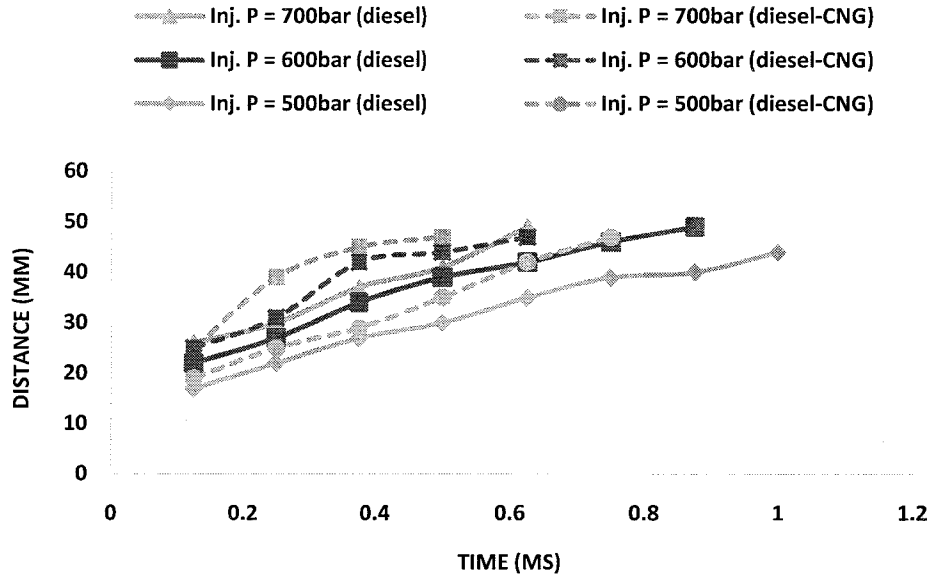


Figure 4.24: Effect of injection pressure on the radial penetration of diesel and diesel-CNG dual fuel impinged on the wall at diesel and CNG injection pressures 600 bar and 18 bar respectively.

4.2.6.2 The effect of wall distance from the injector on the jet radial penetration

Fig. 4.25 and fig 4.26 show the effect of distance from the injector to the wall (80, 60 and 40 mm) on the diesel and diesel-CNG dual fuel radial penetration along the wall respectively. It can be seen that both the diesel (single fuel) and the diesel-CNG dual fuel have a smaller radial penetration at a longer wall distance. This is because the jet velocity becomes lower as it moves downstream. In comparison to the diesel and the diesel-CNG dual-fuel, the wall distance had a higher effect on the pure diesel spray than that of the dual fuel. This is probably caused by the effect of the CNG in the axial direction which enhanced the diesel spray. Also, it can be seen that the differences in the radial penetration between the wall distance of 80 mm and 60 mm is small in comparison to the differences between wall distance of 60 mm and 40 mm. The reason is because the impinging velocities of the jet decreased rapidly in the axial direction until it reached 40 mm in comparison to the decrease in the velocity beyond this distance. These results were found to be in agreement with both findings of Park and Lee [50] and Lee and Lee [66].

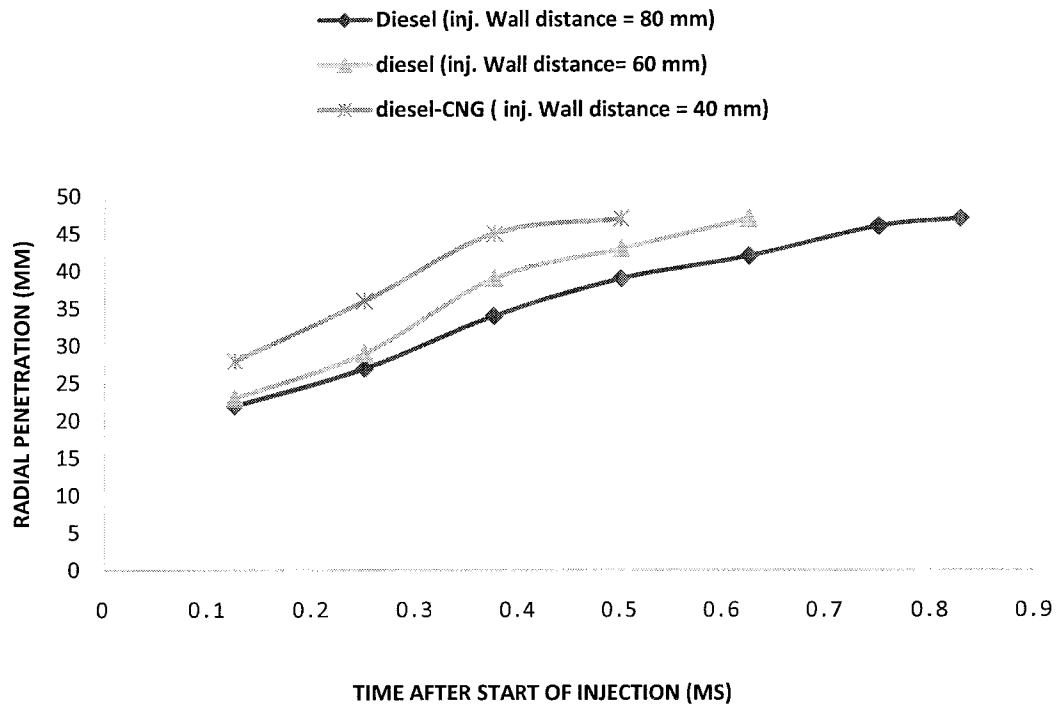


Figure 4.25: Effect of injector-wall distance on the radial penetration of the diesel spray at injection pressure 600 bar.

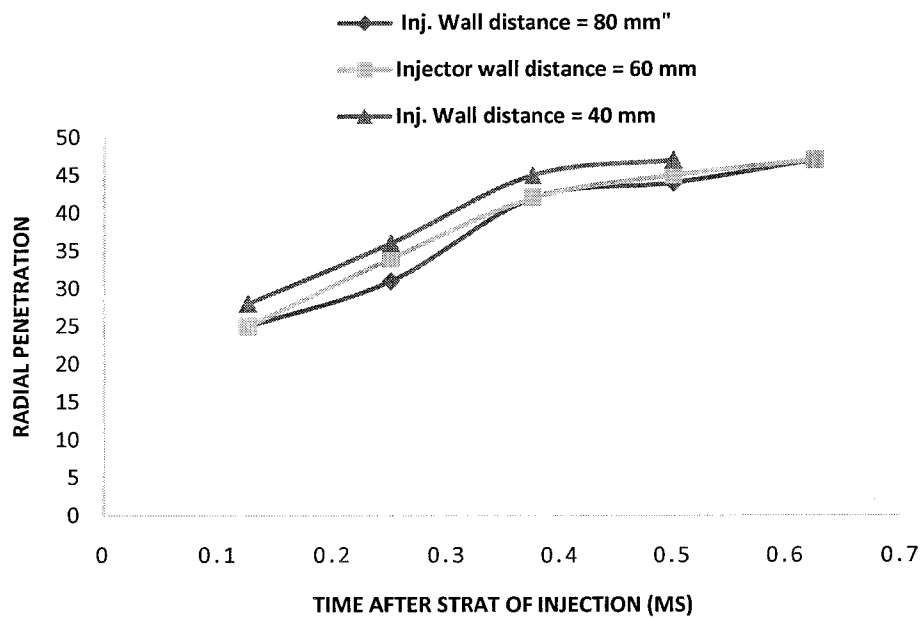


Figure 4.26: Effect of injector-wall distance on the radial penetration of the diesel-CNG dual fuel jet at injection pressure 600 bar and 18 bar respectively.

4.2.6.3 The effect of wall temperature on the diesel and diesel-CNG dual fuel radial penetration

The spray radial penetration along the wall of the diesel and diesel-CNG dual fuel under different wall temperatures (300, 400 and 500° K) are given in Fig. 2.24 and Fig. 2.25. As shown in these figures, as expected, both single and dual fuel radial penetrations were slightly longer at higher wall temperature because the ambient gas density decreased with an increase in the ambient temperature [66]. As time elapsed, the temperature effects were higher in pure diesel spray than that of the dual fuel. This is due to the larger mass of the diesel-CNG dual fuel which resulted in lower temperature effect.

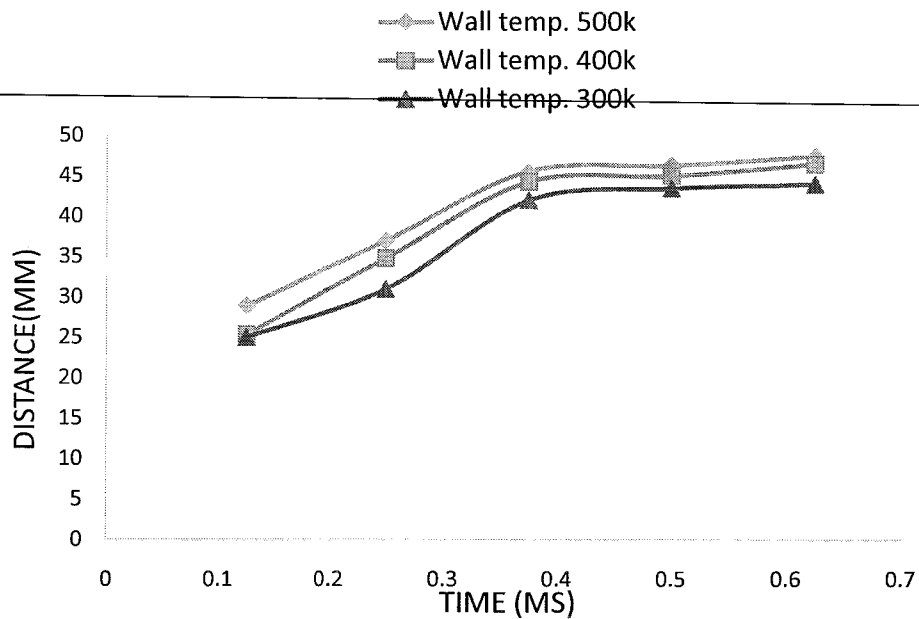


Figure 4.27: Effect of wall temperature on the radial penetration of diesel-CNG dual fuel impinged on the wall at diesel and CNG injection pressures 600 bar and 18 bar respectively.

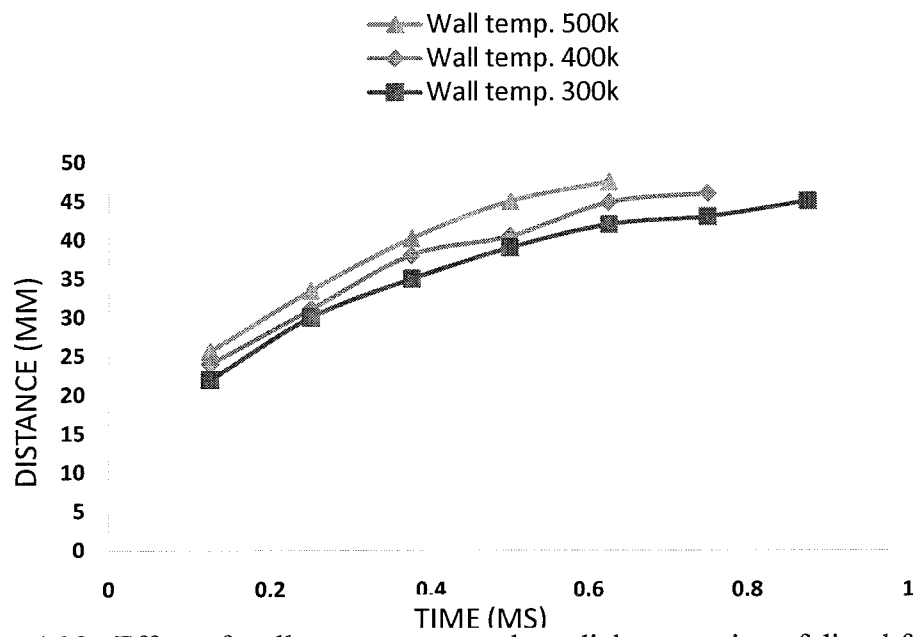


Figure 4.28: Effect of wall temperature on the radial penetration of diesel fuel impinging on the wall at injection pressure 600 bar.

SCHLIEREN IMAGES

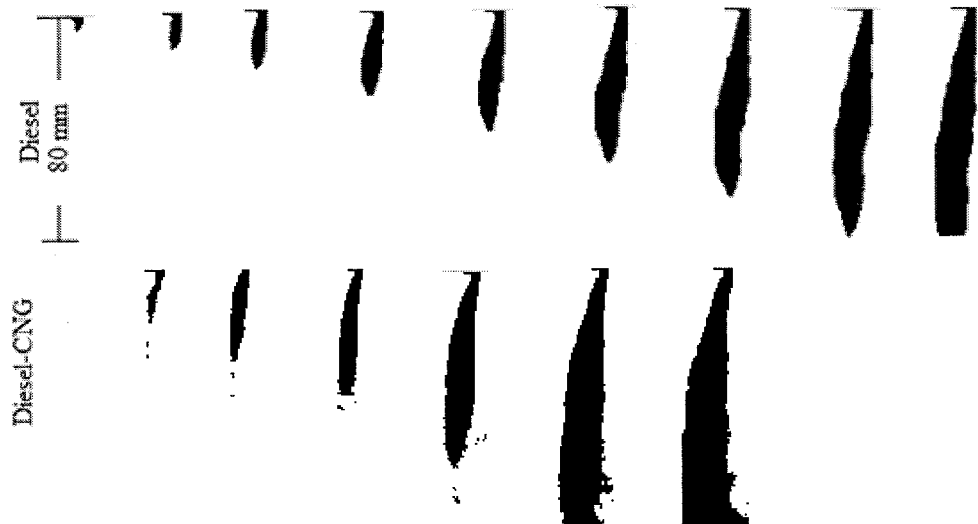
Injection pressure = 700bar



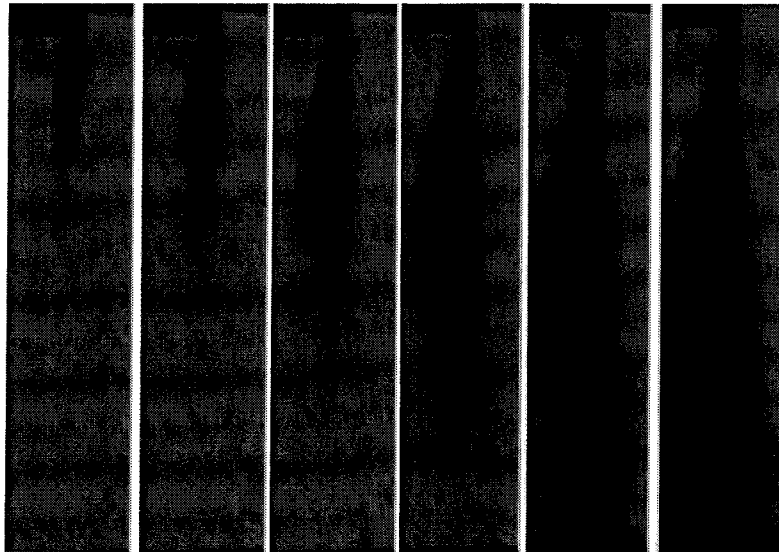
Injection pressure = 800bar



0.125ms 0.25ms 0.375ms 0.5ms 0.625ms 0.75ms 0.875ms 1ms 1.125ms



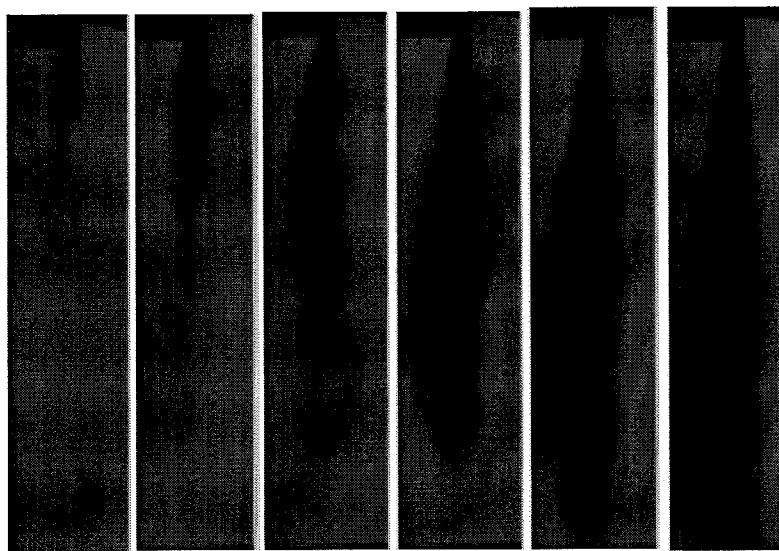
Diesel-CNG 300K



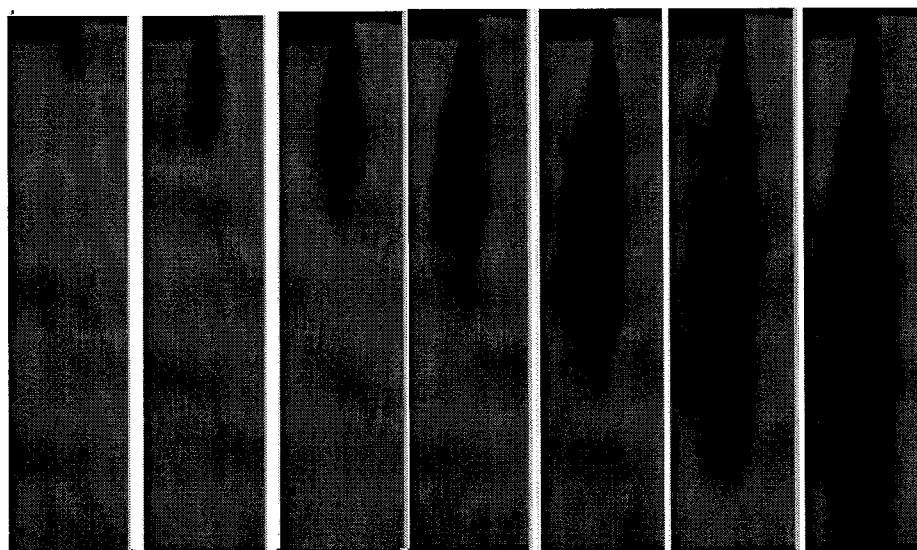
Diesel 300K



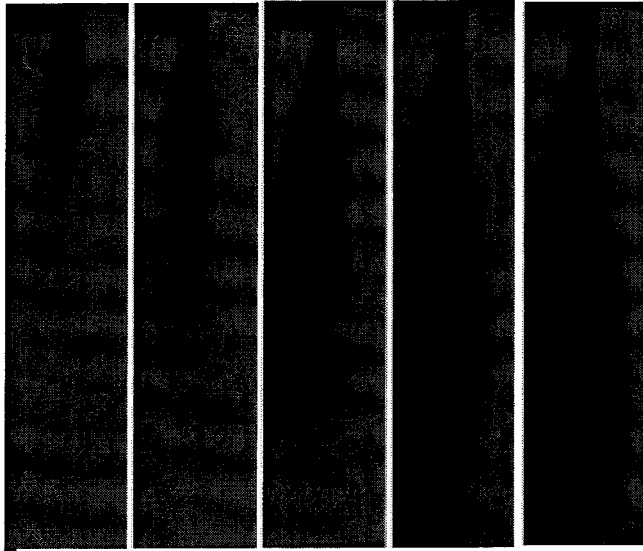
Diesel-CNG 400K



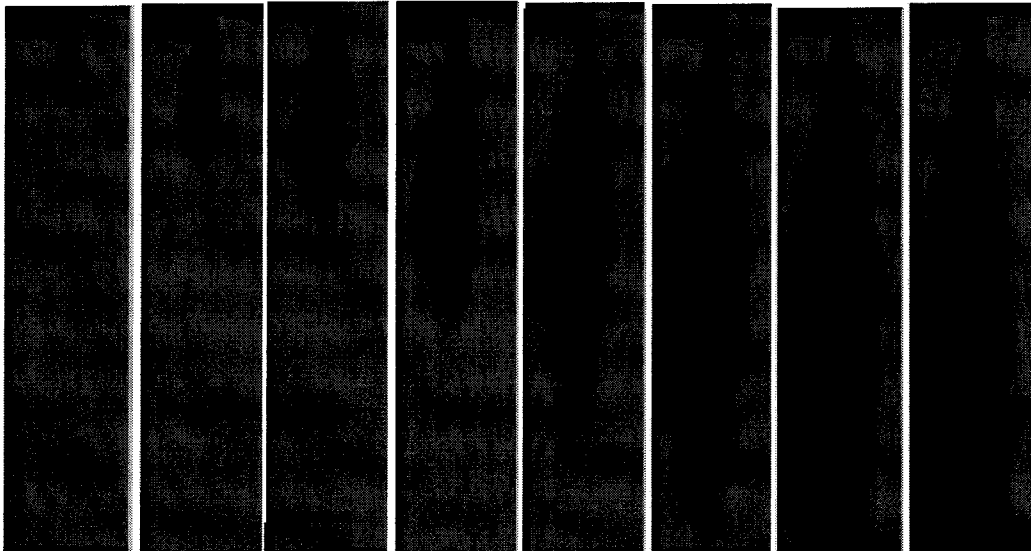
Diesel 400K

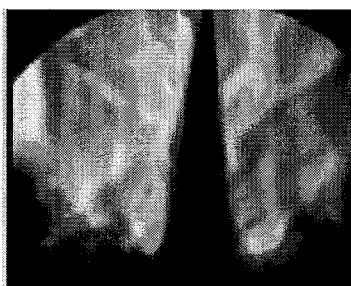
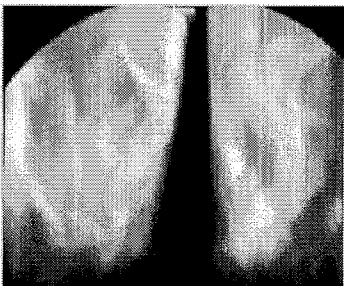
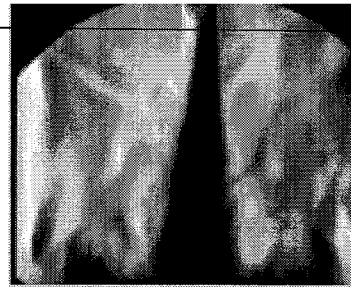
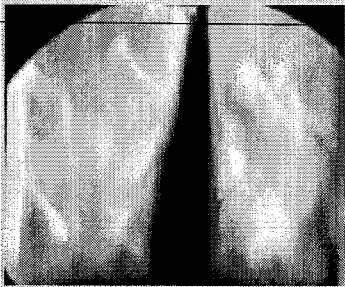
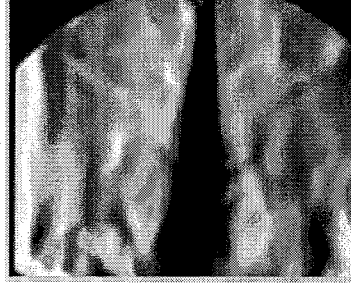
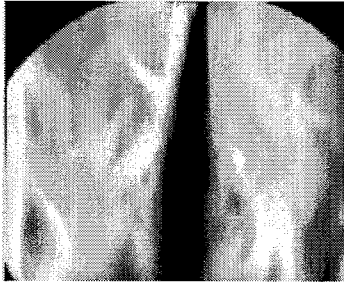
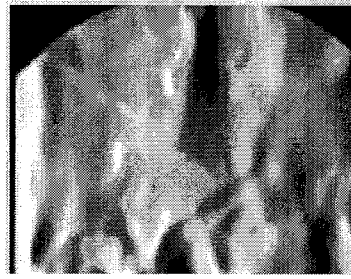
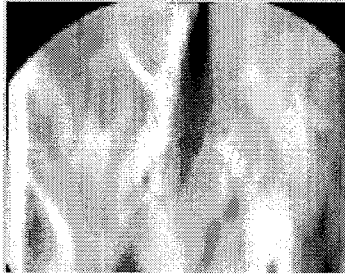


Diesel-CNG 500K



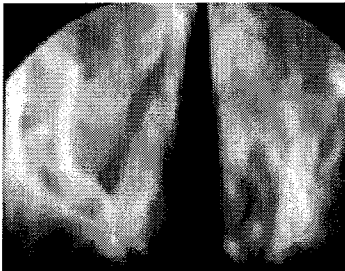
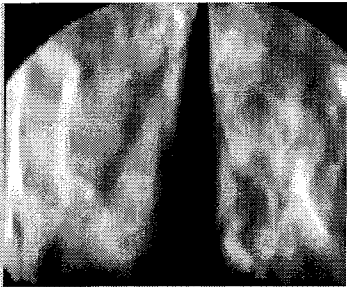
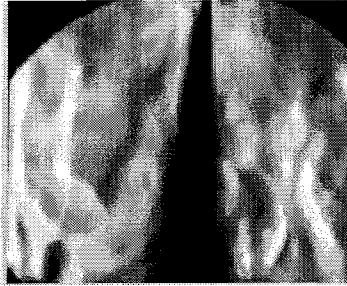
Diesel 500K





Diesel-CNG Impingement 300K

Diesel-CNG impingement 400K



Diesel-CNG impingement 500K

CHAPTER 5

CONCLUSIONS AND RECOMENDATIONS

5.1.1 CONCLUSIONS

Two types of injectors have been used to characterize the propagations of CNG jets and Diesel-CNG dual-fuel jets namely a CNG electronic injector and a high pressure common rail diesel injector. Both fuels were injected into a constant volume chamber ~~at ambient pressure and the Schlieren technique was used to visualize the gas jet~~ propagation, diesel spray and the combination of them. The captured images were processed in order to calculate a number of spray characteristics such as the spray tip penetration, spray cone angle, and spray tip velocity. The spray along the wall which included the radial and its height (thickness) was also measured. The first experiment was to investigate the CNG jet characteristics and its jet wall impingement. The second experiment was to visualize the characteristics of diesel and diesel-CNG dual-fuel and to investigate the effect of CNG on diesel pilot spray. The chosen threshold level was kept to be constant for both cases of diesel single fuel and diesel-CNG dual-fuel while the experimental condition remained constant. Finally, the following conclusions were obtained based on the investigation.

- The CNG jet penetration rate was found to be largely affected by the ambient pressure at the beginning of injection for low injection pressure and short injector-wall distance.
- The CNG jet travel along the wall in both radial and height directions were found to be significantly affected by injection and ambient pressure.
- The penetration rate of the diesel spray was largely influenced by the CNG jet in the axial direction rather than the radial direction. The effect resulted in

higher penetration rate with lower jet cone angle than that of the pure diesel spray.

- The effect of diesel injection pressure on the dual fuel injection was not as significant as compared to the pure diesel spray.
- The penetration rate of diesel-CNG dual-fuel jet was influenced slightly by the ambient temperature as compared to the pure diesel spray. On the other hands, the spray cone angles of the single and dual-fuel did not show significant differences.
- The spray tip velocity of diesel was largely enhanced by the effect of CNG jet and this resulted in higher velocity as compared to the pure diesel spray. While for the case of different ambient temperatures, the spray tip velocity of two injection phases were found to be almost independent on the temperature as compared to the diesel spray.
- For the jet wall-impingement, the diesel-CNG dual-fuel was observed to be higher penetration as compared to pure diesel fuel. On the other hands, the diesel spray was observed to be largely affected by the wall temperature in comparison to the diesel-CNG dual fuel.

5.2 RECOMMENDATIONS

The present research has contributed towards the visualization of CNG jet and diesel-CNG dual fuel jet propagation characteristics as well as the prediction of injection pressure and wall temperatures. However, there is still a need to continue the experimental works in order to achieve further improvements in their characteristics.

Based on the image analysis of Schlieren visualization technique, the CNG propagation cannot be detected while being injected with diesel spray. On the other hand, the diesel pilot characteristics could be enhanced when injected with CNG fuel. However, the jet penetration rate of diesel-CNG dual fuel was found to increase, while the spray cone angle decreased and this was not desirable. Based on these findings, the following recommendations are brought forward for the improvement in the future work:

- It is necessary to investigate the initial development of the CNG jet on the two-phase transit jets. The visualization can be done using planar laser-induced fluorescence (PILF) technique, because it can be accurately used to determine the CNG propagation in the two-phase fuel (diesel-CNG).
- Diesel-CNG dual fuel direct-injection should be investigated in the conditions where it is possible to vary their injectors' angle, thus having opportunity to increase their jets cone angle while determining the mixture formation.
- Diesel-CNG dual-fuel jets should be investigated in a pressurized chamber, in order to have an opportunity to characterize the effects of ambient pressure on their macroscopic characteristics.

REFERENCES

- [1] S. Schneider, "The greenhouse effect: science and policy," *Science*, vol. 243, p. 771, 1989.
- [2] Y. S. H. Najjar, "Alternative Fuels for Spark Ignition Engines," *The Open Fuels & Energy Science Journal*, vol. 2, no. 1, pp. 1–9, Apr. 2009.
- [3] L. Bag, "A Technical Review of Compressed Natural Gas as an Alternative Fuel for Internal Combustion Engines Semin , Rosli Abu Bakar Automotive Excellent Center , Faculty of Mechanical Engineering ,," vol. 1, no. 4, pp. 302–311, 2008.
- [4] T. F. Yusaf, D. R. Buttsworth, K. H. Saleh, and B. F. Yousif, "CNG-diesel engine performance and exhaust emission analysis with the aid of artificial neural network," *Applied Energy*, vol. 87, no. 5, pp. 1661–1669, May 2010.
- [5] T. Korakianitis, "Natural-gas fueled spark-ignition (SI) and compression-ignition (CI) engine performance and emissions," *Progress in Energy and Combustion Science*, vol. 37, no. 1, pp. 89–112, Feb. 2011.
- [6] E. Ramjee, K. V. K. Reddy, B. S. P. Kumar, and M. S. Basha, "Analysis of Emission characteristics on Compression Ignition Engine using Dual Fuel Mode for Variable Speed," vol. 4, no. 3, pp. 23–27, 2012.
- [7] N. J. Birger, "Flow Characteristics of Gas-Blast Fuel Injectors For Direct-Injection," in *Mechanical Engineering*. MSc Thesis: University of British Columbia, 2010.
- [8] L. I. Bo, L. I. Yunqing, and W. Defu, "Spray impingement characterization of a swirl type injector for gasoline direct injection engines," *International Technology and Innovation Conference 2009 (ITIC 2009)*, pp. 1–6, 2009.
- [9] P.-C. Chen, W.-C. Wang, W. L. Roberts, and T. Fang, "Spray and atomization of diesel fuel and its alternatives from a single-hole injector using a common rail fuel injection system," *Fuel*, vol. 103, pp. 850–861, Aug. 2012.
- [10] Ö. O. Taşkiran and M. Ergeneman, "Experimental Study on Diesel Spray Characteristics and Autoignition Process," *Journal of Combustion*, vol. 2011, pp. 1–20, 2011.
- [11] Y. M. Arifin and M. Arai, "The effect of hot surface temperature on diesel fuel deposit formation," *Fuel*, vol. 89, no. 5, pp. 934–942, May 2010.
- [12] J. Lacoste, C. Crua, M. Heikal, D. Kennaird, and M. Gold, "PDA characterisation of dense Diesel sprays using a common-rail injection system," *SAE Technical Paper 2003-01-3085*, 2003.
- [13] R. Bakar and K. Kadirgama, "Application of Natural Gas for Internal Combustion Engines," *cdn.intechopen.com*, pp. 454–475, 2007.

- [14] Y. Liu, J. Yeom, and S. Chung, "A study of spray development and combustion propagation processes of spark-ignited direct injection (SIDI) compressed natural gas (CNG)," *Mathematical and Computer Modelling*, pp. 1–17, Jul. 2011.
- [15] R. Thring, "Alternative fuels for spark ignition engines," *The Open Fuels & Energy Science Journal*, vol. 2, no. 1, pp. 1–9, Apr. 1983.
- [16] M. I. Jahirul, H. H. Masjuki, R. Saidur, M. a. Kalam, M. H. Jayed, and M. a. Wazed, "A Comparative engine performance and emission analysis of CNG and gasoline in a retrofitted car engine," *Applied Thermal Engineering*, vol. 30, no. 14–15, pp. 2219–2226, Oct. 2010.
- [17] K. Kato, K. Igarashi, and M. Masuda, "Development of Engine for Natural Gas Vehicle," *SAE Technical Paper* no. 724, 1999.
- [18] A. C. Chepakovich, "visulization of transit single and two-phase jets creaeted diesel engine injectors," in Mechanical Engineering Departmen, MSc Thesis: university of british columbia, 1993.
- [19] M. Mbarawa, B. Milton, and R. Casey, "Experiments and modelling of natural gas combustion ignited by a pilot diesel fuel spray," *International Journal of Thermal Sciences*, vol. 0729, pp. 927–936, 2001.
- [20] R. Chandra, "Emission Study of CNG Substituted Diesel Engine under Dual Fuel Mode," *Scholars Journal of Engineering and Technology (SJET)*, vol. 1, no. 1, pp. 1–3, 2013.
- [21] O. M. I. Nwafor, "Knock characteristics of dual-fuel combustion in diesel engines using natural gas as primary fuel," *Sadhana*, vol. 27, pp. 375–382, 2002.
- [22] C. A. Laforet, B. S. Brown, S. N. Rogak, and S. R. Munshi, "Compression ignition of directly injected natural gas with entrained diesel," *International Journal of Engine Research*, vol. 11, pp. 207–218, 2010.
- [23] B. S. Brown, C. a. Laforet, S. N. Rogak, and S. R. Munsh, "Comparison of injectors for compression ignition of natural gas with entrained diesel," *International Journal of Engine Research*, vol. 12, no. 2, pp. 109–122, Apr. 2011.
- [24] B. Douville, B., Ouellette, P., Touchette, A., and Ursu, "Performance and Emissions of a Two-Stroke Engine Fueled Using High-Pressure Direct Injection of Natural Gas," *Performance and Emissions of a Two-Stroke Engine Fueled Using High-Pressure Direct Injection of Natural Gas*, vol. Paper 9811, 1998.
- [25] S. Munshi, P. Ouellette, and J. Harrington, "Direct Injection of Natural Gas in a Heavy-Duty Diesel Engine," *SAE Technical Paper 2002-01- 1630*, 2002.
- [26] D. Kennaird, C. Crua, J. Lacoste, and M. Heikal, "In-cylinder penetration and break-up of diesel sprays using a common-rail injection system," *SAE Technical Paper 2002-01-1626*, 2002.

- [27] O. Armas, C. Mata, and S. Martínez-Martínez, "Effect of diesel injection parameters on instantaneous fuel delivery using a solenoid-operated injector with different fuels," *Revista Facultad de*, pp. 9–21, 2012.
- [28] J. Lacoste, "Characteristics of diesel sprays at high temperatures and pressures," School of Engineering. PhD Thesis: University of Brighton, 2006.
- [29] M. Boot, E. Rijk, C. Luijten, B. Somers, and B. Albrecht, "Spray impingement in the early direct injection premixed charge compression ignition regime," *SAE Technical Paper 2010-01-1501*, 2010.
- [30] P. Raghu, "Study on the Spray Characteristics of Diesel and Biodiesel under Non Evaporating Conditions," *European Journal of Scientific Research*, vol. 81, no. 3, pp. 386–396, 2012.
- [31] R. J. H. Klein-Douwel, P. J. M. Frijters, L. M. T. Somers, W. a. de Boer, and R. S. G. Baert, "Macroscopic diesel fuel spray shadowgraphy using high speed digital imaging in a high pressure cell," *Fuel*, vol. 86, no. 12–13, pp. 1994–2007, Aug. 2007.
- [32] E. D. Iffa, a. R. a. Aziz, and A. S. Malik, "Concentration measurement of injected gaseous fuel using quantitative schlieren and optical tomography," *Journal of the European Optical Society: Rapid Publications*, vol. 5, Jun. 2010.
- [33] A. Ghurri, K. Jae-duk, S. Kyu-keun, J. Jae-youn, and K. H. Gon, "Qualitative and quantitative analysis of spray characteristics of diesel and biodiesel blend on common-rail injection system," *Journal of Mechanical Science and Technology*, vol. 25, no. 4, pp. 885–893, 2011.
- [34] X. Helin and Z. Yusheng, "Experimental and Numerical Study on the Characteristics of Liquid Phase LPG and Diesel Fuel Sprays," *Journal of Mechanical Science and Technology*, no. 20020487022, pp. 1–11, 2005.
- [35] A. De Risi, R. Di Sante, and G. Colangelo, "Optical characterization of a Diesel spray at high temperature and pressure," *Technical report, Dipartimento di Ingegneria dell'Innovazione Università degli Studi di Lecce*, pp. 1–13, 2004.
- [36] H. K. Suh, S. W. Park, and C. S. Lee, "Effect of piezo-driven injection system on the macroscopic and microscopic atomization characteristics of diesel fuel spray," *Fuel*, vol. 86, no. 17–18, pp. 2833–2845, Dec. 2007.
- [37] "PLIF Flow Visualization of Methane Gas Jet from Spark Plug Fuel Injector in a Direct Injection Spark Ignition Engine 2 Spark Plug Fuel Injector," *Proceedings of the 1st WSEAS international conference on Visualization, imaging and simulation*, pp. 35–40, 2008.
- [38] S. Mohammed and E. Iffa, "Spray Characteristic Comparisons of Compressed Natural Gas and Hydrogen Fuel using Digital Imaging," *Journal of Applied Sciences.*, pp. 1–5, 2010.
- [39] T. Senoo, M. Sasaki, and M. Shioji, "Spak-ignition stability of natural-gas jets with impingement to cavity walls," *World Automotive Congress*, vol. c, 2010.

-
- [40] J. Yu, H. Hillamo, T. Sarjovaara, and T. Hulkkonen, "Experimental Investigation on Low Pressure Gas Jet Characteristics by Tracer-based PLIF Technique," *Journal of Physics*, pp. 1–14, 2011.
- [41] Yang, "Dual Fuel Compression Ignition Engine," no. 6 August, 2002.
- [42] Y. Shim, G. Choi, and D. Kim, "Numerical Modeling Of Hollow-Cone Fuel Atomization , Vaporization And Wall Impingement Processes Under High Ambient Temperatures," *International Journal of Automotive Technology*, vol. 9, no. 3, pp. 267–275, 2008.
- [43] M. Hamzwhei and M. Rashidi, "Determination of piston and cylinder head temperature distribution in a 4-cylinder gasoline engine at actual process," *Thermal Engineering and Enviroment*, vol. 2006, pp. 153–158, 2006.
- [44] N. Ladommatos, Z. Xiao, and H. Zhao, "The effect of piston bowl temperature on diesel exhaust emissions," *Proceedings of the Institution of Mechanical Engineers, Part D: Journal of Automobile Engineering*, vol. 219, no. 3, pp. 371–388, Jan. 2005.
- [45] C. Pinho, "The positive displacement method for calibration of gas flow meters. The influence of gas compressibility," *Applied Thermal Engineering*, vol. 41, pp. 111–115, Aug. 2012.
- [46] Z. Huang, J. Wang, B. Liu, K. Zeng, J. Yu, and D. Jiang, "Combustion Characteristics of a Direct-Injection Engine Fueled with Natural Gas–Hydrogen Blends under Various Injection Timings," *Energy & Fuels*, vol. 20, no. 4, pp. 1498–1504, Jul. 2006.
- [47] R. Lillington, "A Review of Heavy Duty Diesel Injector Characterization," *Technical report*, pp. 1–19, 2011.
- [48] A. Liaquat and M. Kalam, "Engine Performance and Emissions Analysis using 'Envo Diesel' and Coconut Biodiesel Blended Fuel as Alternative Fuels," *IPCBE*, vol. 6, pp. 168–172, 2011.
- [49] A. Jeronimo and V. Van Der Haegen, "Schlieren Technique – Lab Notes," *EUROAVIA Symposium-Mission to Mars-November-Von Karman Institute for Fluid Dynamics*, pp. 1–15, 2002.
- [50] S. Park and C. Lee, "Macroscopic and microscopic characteristics of a fuel spray impinged on the wall," *Experiments in fluids*, vol. 37, no. 5, pp. 745–762, Sep. 2004.
- [51] J. Shao, Y. Yan, and S. Member, "Digital Imaging Based Measurement of Diesel Spray Characteristics," *Instrumentation*, vol. 57, no. 9, pp. 2067–2073, 2008.
- [52] Taghi Karmipناه, "Application in mixing ventilation Experimental and Numerical Studies," Center for Built Enviroment. PhD Thesis: Royal institute of Technology, 1996.
- [53] Semin, "Injector Nozzle Spray on Compressed Natural Gas Engines: A Technical Review," *International Review of Mechanical Engineerin*, vol. 6, no. 5, p. 5013, 2012.

- [54] N. Zuckerman and N. Lior, "Jet impingement heat transfer: physics, correlations, and numerical modeling," *Advances in heat transfer*, vol. 39, no. 06, pp. 565–631, 2006.
- [55] R. Ding, J. Revstedt, and L. Fuchs, "LIF study of mixing in circular impinging jets effects of boundary conditions," *Proceedings of PSFVIP-4 (Chamonix) F 4015*, pp. 1–13, 2003.
- [56] J. Yu, H. Hillamo, V. Vuorinen, T. Sarjovaara, O. Kaario, and M. Larmi, "Experimental investigation of characteristics of transient low pressure wall-impinging gas jet," *Journal of Physics: Conference Series*, vol. 318, no. 3, p. 032047, Dec. 2011.
- [57] B. C. Lionel Martinez, Adl'ene Benkenida, "A Study of the Diesel Spray Dynamics using Eulerian-Eulerian large eddy simulation," pp. 1–38, 2010.
- [58] F. Wåhlin, "Experimental Investigation of Impinging Diesel Sprays for HCCI Combustion," Department of Mechine Design, PhD Thesis: Royal Institute of Technology, 2007.
- [59] X. Jiang and G. Siamas, "Physical modelling and advanced simulations of gas–liquid two-phase jet flows in atomization and sprays," *Progress in Energy and Combustion Science*, vol. 36, pp. 131–167, 2010.
- [60] I. Pribicevic and T. Sattelmayer, "Investigation of the Diesel spray atomization process with use of Phase Doppler Anemometry at high injection pressures and at engine-like gas density," *16th Int Symp on Applications of Laser Techniques to Fluid Mechanics*, no. 2003, pp. 9–12, 2012.
- [61] S. Sazhin, W. Abdelghaffar, E. Sazhina, and M. Heikal, "Models for droplet transient heating: Effects on droplet evaporation, ignition, and break-up," *International Journal of Thermal Sciences*, vol. 44, no. 7, pp. 610–622, Jul. 2005.
- [62] A. Magnusson and S. Andersson, "An Experimental Study of Heat Transfer between Impinging Single Diesel Droplets and a Metal Wall using a Surface Mounted Height Adjustable Rapid Thermocouple," *24th European Conference on Liquid Atomization and Spray Systems*, no. September, pp. 1–7, 2011.
- [63] H. Hiroyasu, and M., Arai, "Structures of Fuel Sprays in Diesel Engines," *SAE Paper NO. 900475*, 1990.
- [64] J.C.Dent, "A Basis for the comparison of various experimental methods for studying spray penetration," in *SAE Paper NO. 710571*, 1971.
- [65] H. Hiroyasu, "Diesel engine combustion and its modeling," in *proceeding of the international symposium on diagnostics and modeling of combustion in Reciprogating engines*, pp. 53–75, 1985.
- [66] C. H. Lee and K. H. Lee, "Experimental Study On Macroscopic Spray Characteristics After Impingement In A Slit-Type Gdi Injector," *International Journal*, vol. 9, no. 3, pp. 373–380, 2008.

APPENDIX A

MATLAB IMAGING CODE

1. Image Processing Code

```
%% Define External parameters
% Boundary detection
% Read the Image

Image = imread('.jpg');

% split the display into 3 rows and one column
subplot(221);
% display the image in the first row
imshow(Image(:,:,1));
title('Original Image');



---


% convert the image to gray scale
ImageGray = rgb2gray(Image(:,:,end,:));
% display the gray image in the second row
subplot(222);
imshow(ImageGray, []);
title('Grayscale Image');

%% Post processing step
% split the image into two regions at column 345 and crop
it from the left
% at column 300 and from the right at column 400
ImageLeft = im2bw (ImageGray(:,:,1),0.);
subplot(223)
imshow (ImageLeft),
title('left image');
ImageRight = im2bw(ImageGray(:,:,2), 0.);
subplot(224)
imshow (ImageRight),
title('Right image');
% Merge the left and right images into one image
NewImage = cat(2, ImageRight,ImageLeft);
% display the combined image
subplot(221);
imshow(NewImage);
title('Binary Image');

%% Computing angle
% edge contour for right side
% Search for all rows
```



```

RightContour = [];
for i = 1:size(NewImage,1)
    % Extract raw(i) data
    a = NewImage(i,:end);
    % find the 1st derivative of a
    b = diff(a);
    % find the nonzero derivative
    idx = find(b ~= 0);
    % if there is more than one point take the furthest
one
    if length(idx) > 1
        idx = max(idx);
    end
    if ~isempty(idx)
        RightContour(i) = idx;
    else
        RightContour(i) = 0;
    end
end

% plot the edge contour
figure(2);
subplot(221);
plot(1:size(NewImage, 1), RightContour);
title('Right edge contour');

% smoothing the edge contour
RightContourSmoothed =
filter(ones(1,WindowSize)/WindowSize, 1, RightContour);
subplot(223);
plot(1:size(NewImage, 1), RightContourSmoothed);
title('Smoothed right side edge contour');

% edge contour for left side
% Search for all rows
LeftContour = [];
for i = 1:size(NewImage,1)
    % Extract raw(i) data
    a = NewImage(i,:);
    % find the 1st derivative of a
    b = diff(a);
    % find the nonzero derivative
    idx = 33- find(b ~= 0);
    % if there is more than one point take the furthest
one
    if length(idx) > 1
        idx = max(idx);
    end
    if ~isempty(idx)
        LeftContour(i) = idx;
    end
end

```

```

        else
            LeftContour(i) = 0;
        end
    end
end
% plot the edge contour
subplot(222);
plot(1:size(NewImage, 1), LeftContour);
title('Left edge contour');
% smoothing the edge contour
LeftContourSmoothed =
    filter(ones(1,WindowSize)/WindowSize, 1, LeftContour);
subplot(224);
plot(1:size(NewImage, 1), LeftContourSmoothed);
title('Smoothed left side edge contour');

%% Plot the cone
figure(3);
% plot the cone before smoothing
subplot(121);
plot(1:size(NewImage, 1), RightContour, 'b');


---


hold on;
plot(1:size(NewImage, 1), -LeftContour, 'r');
plot([], [], [RightContour(), RightContour()], '--g');
plot([], [], [-LeftContour(), -LeftContour()], '--g');
hold off;
title('Edge contour before smooting');

% plot the cone after smoothing
subplot(122);
plot(1:size(NewImage, 1), RightContourSmoothed, 'b');
hold on;
plot(1:size(NewImage, 1), -LeftContourSmoothed, 'r');
plot([], [], [RightContourSmoothed(),
    RightContourSmoothed()], '--g');
plot([], [], [-LeftContourSmoothed(), -
    LeftContourSmoothed()], '--g');
hold off;
title('Edge contour before smooting');

%% compute the angles
ptr = [+RightContourSmoothed(), ];
ptl = [-LeftContourSmoothed(), ];
pbr = [+RightContourSmoothed(), ];
pbl = [-LeftContourSmoothed(), ];
AngleRight = 90 - abs(atan2((pbr(2)-ptr(2))/(pbr(1)-
    ptr(1)))));
AngleLeft = 90 - abs(atan2((pbl(2)-ptl(2))/(pbl(1)-
    ptl(1)))));
ConeAngle = AngleRight + AngleLeft

```

%% Compute Vertical distance

```
DepthRightSide = find(RightContourSmoothed > , , 'last' );  
DepthLeftSide = find(LeftContourSmoothed > , , 'last' );  
FlameDepth = mean([DepthRightSide, DepthLeftSide])
```

%% Radial distance

```
RadialDistance = abs(RightContourSmoothed(end) +  
LeftContourSmoothed(end))
```

%% Height distance

```
if RadialDistance > 10  
    HeightRight = size(RightContour,2) -  
    find(RightContourSmoothed > ...  
        RightContourSmoothed(end), 1, 'last' );  
    HeightLeft = size(LeftContour, 2) -  
    find(LeftContourSmoothed > ...  
        LeftContourSmoothed(end), 1, 'last' );  
    Height = max([HeightRight, HeightLeft])  
End.
```